Topological phenomena in quantum gases

Jérôme Beugnon

Habilitation à diriger des recherches de Sorbonne Université

préparée par Jérôme BEUGNON

Gaz quantiques et topologie

Topological phenomena in quantum gases

Soutenue le 11 Octobre 2018 devant le jury composé de :

M. Rudolf GRIMM ..... Rapporteur
M. David GUÉRY-ODELIN ..... Rapporteur
Mme Laurence PRUVOST ..... Rapporteur
Mme Leticia CUGLIANDOLO ..... Examinatrice (Présidente du jury)
M. Pascal SZRIFTGISER ..... Examinateur
M. Peter van der STRATEN ..... Examinateur

Travail réalisé au laboratoire Kastler Brossel, site du Collège de France.

Contents

Introduction

In this manuscript, I describe my research activities on ultracold Bose gases since I joined the Bose-Einstein condensate team of Laboratoire Kastler Brossel (LKB) in 2008. Prior to this work I have been a postdoctoral fellow at Laboratoire Aimé Cotton where I studied resonant interactions between Rydberg atomic pairs in an atomic beam. A description of the main results we obtained can be found in Ref. [1]. At LKB, I first started to work on the *metastable helium project* with Michèle Leduc for two years and then I initiated with Fabrice Gerbier the ongoing *artificial magnetism in optical lattices project* with ytterbium atoms in 2009. More recently, since 2011, I am also involved in the *two-dimensional Bose gas project* together with Jean Dalibard and Sylvain Nascimbene. This project first started on the existing setup at Ecole Normale Supérieure and is now continuing on a new setup at Collège de France where all our team and experiments are installed since 2014.

Quantum physics in the 21st century

The development of quantum physics within the last 100 years has opened a very broad field of research including now, for instance, chemistry, solid-state physics, particle and nuclear physics, atomic and molecular physics, astrophysics and cosmology... Quantum physics is a the heart of a large part of the worldwide basic research activities and provides huge challenges (i) on the theory side because of the exponentially increasing size of the Hilbert space with the system size and the important role of correlations (entanglement) between different parts of this space; (ii) on the experimental side because of the difficulty to handle systems well-preserved from decoherence while maintaining a high degree of control.

More recently, quantum physics and quantum materials have been put to the forefront as good candidates to overcome some global challenges that our world will have to face in this century [2, 3] and which maybe require groundbreaking advances. Among others quantum computers are expected to solve efficiently problems relevant for instance for artificial intelligence or more generally for optimization protocols. Quantum simulators may offer suitable tools to understand and develop new phases of matter, like high-temperature superconductors thus enabling a better management of energy. On the same topic, quantum materials, like solar cells could provide more efficient and durable light harvesting techniques. Safe exchanges through communication channels may also benefit from the intake of quantum cryptography and communications.

Most of the technical progresses in these directions are expected to come from condensed-matter physics and photonics, which are the best candidates for practical implementations. However, fundamental research of well-controlled and tunable systems is also crucial and the field of ultracold quantum gases provides such systems where a deep understanding and an extreme versatility are possible.

Ultracold quantum gases

Whereas Fermi gases of electrons are extensively studied in condensed-matter physics since the early days of quantum physics, Bose gases are less common. The paradigmatic example of liquid helium, first observed in 1908, has for a long time been the only playground to study Bose systems. An impressive amount of results on this system have been reported like the observation of superfluidity (1911), quantum

vortices or the normal to superfluid Berezinskii-Kosterlitz-Thouless (BKT) transition in two-dimensional systems [4]. Bose-Einstein condensation plays a crucial role for this system but strong interactions between particles hinder the pure effect of quantum statistics.

The realization of Bose-Einstein condensation in dilute atomic gases in 1995 has renewed the interest on Bose gases because of the possibility to study weakly interacting systems and make quantitative comparison with models [5, 6]. The demonstration of superfluidity and quantized vortices quickly followed [7, 8, 9]. The dynamics of trapped Bose-Einstein condensates (BECs) have been accurately investigated and demonstrated the validity of the Bogoliubov microscopic description [10]. Gaseous BECs have been followed in 2001 by ultracold Fermi gases [11], which provide a fruitful alternative to condensed-matter systems.

Thanks to the fast development of laser technologies, we are now able to manipulate ultracold quantum gases in optical dipole traps with a great versatility. First, one can change the dimension of the system by strongly confining atoms along one or two directions of space to create two-dimensional and one-dimensional gases [12]. Thanks to beam shaping techniques it is also possible to draw arbitrary potentials on the atomic clouds [13, 14, 15, 16, 17, 18, 19]. Finally, by making two beams interfere, one can create periodic potentials, the so-called optical lattices, in which particles are trapped in great analogy with electrons in solid-state devices [20]. In addition to the flexibility for the confinement, interactions between particles can be controlled thanks to Feshbach resonances [21]. Last, the interaction with the environment can be almost fully cancelled leading to the realization of well-defined closed systems or, alternatively, this interaction can be tailored at will to study the dynamics of quantum open systems [22].

Topological phenomena in quantum gases

Topology is playing an increasing role in physics. Besides the mathematical elegance of the topological understanding of some physical phenomena, the great importance of topology in physics usually stems from the robustness of topological properties for instance to defects or geometrical deformations. The topological robustness is expected to be crucial for the emergence of quantum devices like for instance, Majorana fermions for quantum computing [23] or topological lasers [24, 25, 26].

Topology is well-known in the study of superfluids. For instance, vortices are topological defects which are characterized by an integer winding of the phase of the wavefunction around the vortex core. Topology is also at the heart of the Berezinskii-Kosterlitz-Thouless (BKT) phase transition to a superfluid state in 2D [27]. It is a topological phase transition, very different from continuous phase transitions, where the transition is associated to a change in the topology of the system. In addition, a large variety of topological defects exists in spinor superfluids [28]. We will explore topological features in superfluids in the two first chapter of this manuscript.

The most celebrated example of interplay between topology and physics is undoubtedly the description of Quantum Hall Effect (QHE) in two-dimensional electron gases [29]. In this case, the quantization of transverse conductivity is associated to a topological number (the Chern number) which characterizes the topology of the band structure. To explore similar physics with ultracold atoms one needs to simulate orbital magnetism *i.e.* the effect of a magnetic field on the motion of charged particles. This goal has motivated an intense theoretical activity to propose protocols to implement this artificial magnetism using for instance rotation of the cloud [30], light-induced potentials [31], time-modulation of optical lattices or light-induced complex tunnelling [32]. Very recently, topological band structures have been realized in some pioneering experiments [32]. In our team, we aim at applying the protocol described in [33, 34] and I will describe our work in the direction of the quantum Hall effect with bosons in the last chapter of this thesis.

Present and future of ultracold quantum gases

A great challenge for the future in the quantum gases field is to use all these degrees of freedom to investigate the physics of many-body systems in non-trivial configurations where the role of interactions, topology and the interplay between both (like in the Fractional Quantum Hall Effect) can be controlled to realize rich and yet unexplored phases of matter. These investigations will be developed in parallel with theory progress to benchmark the ability to get reliable results and to prove that ultracold quantum gases can be used as robust quantum simulators. Whereas all the aforementioned interesting features of quantum gases have been demonstrated in several groups, merging many of them efficiently on a single experimental apparatus is getting increasingly difficult and requires state-of-the-art technologies and highly-trained teams. Many of the targeted breakthroughs may also be limited in the near future by the too high temperatures/entropy commonly achieved in experiments (on the range of tens of nK) which are comparable to energy gaps of the studied many-body phases. Here again laser-shaping of optical traps has been used to make significant progress in this direction allowing the observation of antiferromagnetic interactions in spin chains [35].

In the above description, I have selected only a few topics of the field which are lying in the context of this manuscript but ultracold quantum gases are also well adapted for many other subjects like localization in disordered potentials [36, 37], molecular physics [38], metrology [39] or quantum information processing.

Main results of this work

In this framework, we aim at contributing to the field with experimental studies on ultracold Bose gases. One project is dedicated to two-dimensional rubidium Bose gases in box-like potentials. The other focuses on the study of artificial magnetism with ytterbium atoms confined in optical lattices and manipulated on an optical clock transition. These two projects correspond to two different experimental setups and teams but they clearly have strong connections.

Two-dimensional Bose gases Most of our work on the two-dimensional Bose gas concerns the dynamical behaviour of the system and the probing of superfluidity and coherence properties using (mostly) recently developed uniform box-trapped gases. We have first initiated the realization of box-like potentials on the existing 2D setup and we have developed a fully new apparatus dedicated to this topic. Thanks to these apparatus we have demonstrated the superfluid character of the gas and studied the propagation of second sound which is also related to the gas superfluid fraction. In addition, we have characterized how coherence is restored after quenching the system to an out-of-equilibrium situation and measured the statistical distribution of the topological defects formed after different kinds of quenches in several geometries.

High-resolution optical spectroscopy of Bose gases We have built a new experimental apparatus to manipulate quantum gases of ytterbium atoms. This two-electron atom has specific properties compared to standard alkali like the presence of an ultranarrow clock transition which is at the heart of our activities and of the protocol that we plan to implement to create artificial magnetism. In this manuscript, I will describe the development of this apparatus and some studies that we have recently realized combining an ultranarrow laser and quantum gases. In these experiments we have probed ytterbium bulk BECs and few-particle systems confined in an optical lattice. These experiments allowed us to fully understand and characterize the rich dynamics of optically-coupled quantum systems.

Outline

The manuscript is organized as follows. I describe in chapter 1 recent results that we have obtained on two-dimensional Bose gases whereas chapter 2 describes the associated research plans. The first achievements on our ytterbium project, mainly about optical spectroscopy of many-body phases with high resolution optical spectroscopy are described in chapter 3 along with our research plans on this setup about artificial magnetism in optical lattices. The manuscript terminates with an overall conclusion.

CHAPTER 1

Two-dimensional Bose gases

1.1 Introduction

The study of quantum gases of bosons in two dimensions is motivated by several reasons. One of the most interesting feature of two-dimensional Bose gases is the existence of a topological phase transition from the high temperature normal phase to a low temperature superfluid state. This phase transition is of BKT (Berezinskii-Kosterlitz-Thouless) type. It is a topological phase transition and its initial description is the subject of the Physics Nobel Prize in 2016 [27]. It has been observed with an ultracold gas in our team in 2006 [40] and studied in several other teams [41, 42, 43, 44].

This specific phase transition is not a symmetry breaking phase transition (as Bose-Einstein condensation for instance) and it features several original properties relevant to describe weakly interacting bosonic gases. Among this properties we wish to emphasize the following ones [45]:

- The low temperature phase is superfluid. The superfluid fraction exhibits a jump at the critical temperature from zero in the normal phase to a finite value in the superfluid phase. This behaviour was observed with liquid helium films [46].
- The low temperature phase, even if superfluid, does not present true long-range order, in agreement with Hohenberg-Mermin-Wagner theorem [47, 48]. In this phase the gas exhibits quasi-long range order corresponding to an algebraic decay of the first-order correlation function. In the normal phase, close to the critical point, quasi-long range order disappears and an exponential decay of the correlation function is predicted.
- The topological character of this phase transition can be understood from a microscopic point of view. The transition from the superfluid phase to the normal phase corresponds to the unbinding of vortex pairs into single vortices. Some signatures of this behaviour have been observed in Ref. [49].

Besides these fundamental properties of the 2D Bose gas, 2D systems also offers clear advantages from an experimental perspective. The main probing technique of quantum gases is absorption imaging. Using single atomic layers allows an efficient characterization of the clouds, possibly with a high optical resolution and without being limited by the depth of focus of the system. High optical resolution can also be used to tailor optical potentials with a good spatial resolution. We have exploited this feature in our team to create custom-shaped flat-bottom potentials using spatial light modulators.

Finally, physics in 2 dimensions of space is particularly suitable to investigate topological phases of matter, as exemplified by quantum Hall physics in 2D electron gases [50].

Most of the results described in this chapter have been reported in several theses realized by students that I have co-supervised [51, 52, 53, 54]. Three other PhD students are currently doing their PhD in our team (R. Saint-Jalm, E. Le Cerf and B. Bakkali). This work also involved several postdoctoral fellows: C. Weitenberg, T. Bienaimé, M. Aidelsburger, P.M. Castilho. This project is conducted in collaboration with S. Nascimbene and J. Dalibard.

1.2 Basic features of 2D Bose gases

In this section we review a few properties of the 2D Bose gas that are of interest for the following of this chapter. Much more comprehensive descriptions can be found in [45, 55].

1.2.1 The 2D Bose gas at zero temperature

In 3D, weakly interacting Bose gases at zero temperature can be well described by the mean-field Gross-Pitaevskii equation. This equation is non-linear because of the presence of interactions between particles which are described by a coupling constant $g = 4\pi a\hbar^2/m$, where a is the s-wave scattering length.

In the following, we will consider a gas to be two-dimensional if the characteristic thermal and interaction energies are smaller than the typical confinement energy along the direction perpendicular to the plane. However, in the regime explored here the typical thickness of the cloud (hundreds of nm) is much larger than the s-wave scattering length (5.3 nm) and collisions in the gas are three-dimensional. In this regime, for low enough temperatures and for a strong harmonic confinement along z, one can show that the wavefunction $\psi(\mathbf{r}, t)$ of a uniform gas is given by an effective 2D Gross-Pitaevskii equation [45]

$$i\hbar\frac{\partial\psi}{\partial t} = -\frac{\hbar^2}{2m}\nabla^2\psi + \frac{\hbar^2}{m}\tilde{g}|\psi|^2\psi. \tag{1.1}$$

Interactions are then described by the dimensionless parameter $\tilde{g} = \sqrt{8\pi}a/l_z$, where $l_z = \sqrt{\hbar/(m\omega_z)}$ is the harmonic oscillator length along the strongly confining z direction. In our experiment we typically explore the regime where $\tilde{g} \approx 0.1 - 0.2$ is small (weakly-interacting regime). Larger values of the interaction parameter have been explored for atoms with an available Feshbach resonance [56] or for molecules in Fermi systems [57, 58].

Starting from this effective 2D situation, it is possible to investigate Bogoliubov excitations in the system [59, 45] in a way similar to what is done in 3D, even if phase fluctuations at $T \neq 0$ could destroy the order parameter at large distances. We obtain the "usual" Bogoliubov spectrum for excitations at wavevector k.

$$E(k) = \sqrt{\frac{\hbar^2k^2}{2m}\left(\frac{\hbar^2k^2}{2m} + \frac{\hbar^2}{m}\tilde{g}n_{2\mathrm{D}}\right)}, \tag{1.2}$$

where $n_{2\mathrm{D}}$ is the surface density of the cloud. For $k \ll \xi^{-1} = \sqrt{\tilde{g}n_{2\mathrm{D}}}$, these excitations are phonons with a Bogoliubov speed of sound $c_B = \sqrt{\hbar^2\tilde{g}n_{2\mathrm{D}}/m^2}$, which is typically a few mm/s in our experiments.

1.2.2 Equation of state

In a weakly interacting 2D Bose gas described by a classical field theory, there is a specific scale invariance. It can be shown that the thermodynamic properties can then be expressed only as a function of the dimensionless combination μ/k_BT and does not depends on μ and T separately. This scale invariance could be understood from the absence of dimension of the interaction parameter $\tilde{g}$, contrary to the 3D case [55].

This scale invariance means that a relatively simple equation of state of the gas can be found. For instance, the knowledge of $\mathcal{D} = f(\mu/k_BT)$, where $\mathcal{D} = n_{2\mathrm{D}}\lambda_T^2$ with $\lambda_T = h/\sqrt{2\pi mk_BT}$ the thermal wavelength, is an equation of state of the system containing the full thermodynamical properties of the gas. This equation of state has been computed with classical field Monte-Carlo simulations in [60] and

confirmed with quantum Monte-Carlo methods [61]. Measurements of the equation of state in Bose gases have been reported in Refs. [56, 62, 63, 64] and measurements in 2D Fermi gases in Refs. [65, 66] and show a good agreement with these predictions.

1.2.3 Coherence properties of the 2D Bose gas

Phase fluctuations and coherence can be characterized by the first order correlation function

$$g_1(\mathbf{r}) = \langle \hat{\Psi}^\dagger(\mathbf{r})\hat{\Psi}(0)\rangle, \tag{1.3}$$

where $\hat{\Psi}$ is the annihilation operator. Depending on the degeneracy of the cloud this function shows very different behaviours [45].

- At high temperature and for an ideal gas, where the gas can be described with Boltzmann statistics, g_1 has a Gaussian shape with a characteristic decay length given by the thermal wavelength λ_T.
- At lower temperature and for an ideal gas, but above the critical point, the correlation function decays exponentially, $g_1(r) \propto e^{-r/\ell}$, at large distances compared to λ_T. The decay length is given by $\ell = \lambda_T e^{\mathcal{D}/2}/\sqrt{4\pi}$. The decay length grows exponentially with $\mathcal{D}$ and can thus become very large[1].
- Below the critical temperature and for an interacting gas, the long-distance behaviour of the correlation length is dominated by the low-energy phonon modes and is given by $g_1(r) \propto r^{-1/\mathcal{D}_s}$, where $\mathcal{D}_s$ is the superfluid fraction phase-space density. This (slow[2]) algebraic decay is the signature of quasi-long range order in this system.

1.3 Experimental realization of 2D Bose gases

1.3.1 Confinement to 2D

The usual approach to realize a 2D Bose gas is to strongly confine a 3D cold atomic cloud along one direction. In our experiments, we usually explore thermal energies and interaction energies on the order of $k_B T, E_{\text{int}} \approx 100\,\text{nK}$. The confinement frequency should thus be on the order of a few kHz to ensure two-dimensionality.

Several techniques are available to realize a 2D Bose gas. A common approach is to use an optical trap to engineer a fast spatial variation of the potential. To obtain a single 2D gas, one can create a single potential minimum [42, 67]. In these cases the confinement is often limited because of the relatively large size of the beam waists (few μm). Another approach is to create an optical lattice by interfering two laser beams [68, 43]. Then, one has to find a trade-off between using a short lattice spacing that enables to reach high confinement energies and using a large lattice spacing, which makes single-plane loading easier. In our team we have first been working with a single repulsive optical potential that was shaped into a Hermite-Gauss mode (with a dark line at its center) [67]. More recently we have designed and implemented an optical accordion lattice trap for which the angle between the interfering beams can be tuned dynamically from a large spacing configuration favouring the loading of atoms around a single node of the lattice to a short lattice spacing favouring a strong confinement. This work is described in [69] and in Fig. 1.1. Finally, another possibility is to use a radio-frequency dressed magnetic potential [70].

[1] Taking into account interactions one can show that ℓ diverges at the critical point, as expected generally for a phase transition, but this divergence is exponential rather than a power-law, as for the case of a second order phase transition.

[2] The exponent for the decay is 1/4 at the transition and gets smaller for more degenerate clouds.

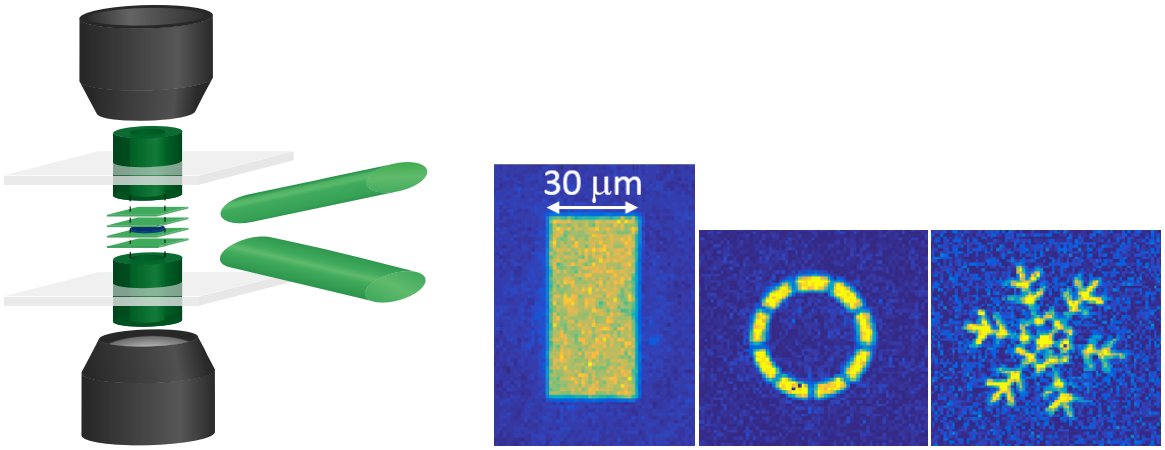

Figure 1.1: *Left: Sketch of the experimental setup. A vertical optical lattice is created thanks to the low-angle interference between two laser beams. A single node of this lattice is loaded with a cold atomic gas. The angle between the two beams can be tuned dynamically to adjust the lattice spacing. Two microscope objectives are place below (for imaging) and above the cloud (for tailoring the in-plane potential). The in-plane potential profile is obtained by direct imaging of the chip of a spatial light modulator. Right: Examples of absorption pictures of atomic clouds. Box, ring-shaped or more complex potentials can be realized and possibly dynamically modified.*

1.3.2 In-plane confinement

The strong confinement along the vertical direction is usually created by a laser with a large waist and is always chosen repulsive in our team. It thus has almost no influence on the in-plane trapping potential. Practically, the decrease of the strength of the confinement away for the center of the trap because of the finite extension of the laser beam leads to an anti-confining potential which is of about a few (imaginary) Hz with our parameters [52].

The shaping of the in-plane trapping potential is flexible. Around 2012, on the ENS setup, we used a harmonic confinement created by a rotating magnetic quadrupole trap (TOP configuration). Then, we started to investigate box potentials at ENS (2013-2015). At Collège de France (2016-now), we still use box potentials but with a much better optical resolution to design the potential (around 1 μm) and with a large flexibility thanks to the use of spatial modulators (see Fig. 1.1). We currently use two digital micro mirror (DMD) devices which allow us to change at will the shape of the trapping potential both between each experimental sequence and during a given sequence by playing movies on the DMD.

Our approach to produce two-dimensional custom-shaped atomic clouds is now used in several other teams studying Bose gases [18, 71] and Fermi gases [72].

1.4 Probing superfluidity and coherence of the 2D Bose gas

1.4.1 Superfluid behavior of the 2D Bose gas

This study is published in Ref. [73] and the full text of the article is reproduced in the appendix.

As discussed in the previous section, the weakly interacting 2D Bose gas is superfluid below the BKT critical temperature. The superfluid density and its jump at the critical point have been measured in liquid helium films [46]. Superfluidity can be defined in several ways but the most intuitive picture is that it allows a dissipation-less motion of the fluid around a defect for low enough relative velocity between the fluid and the defect. In Ref. [73] we have probed this criterion for superfluidity in a 2D Bose

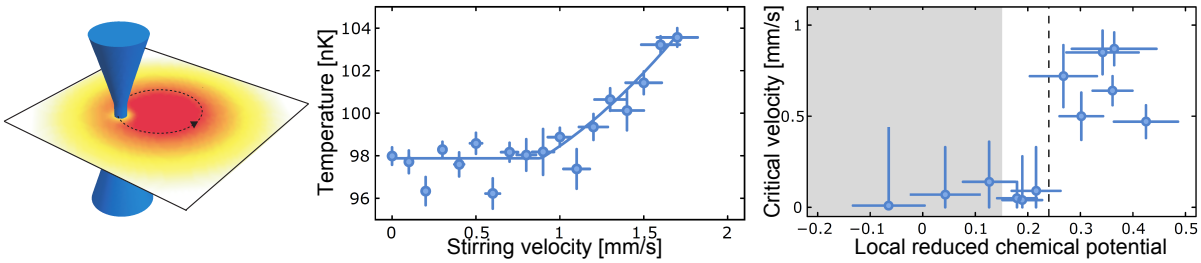

Figure 1.2: *Left: Sketch of the experiment. A 2D cloud of atoms harmonically trapped is stirred by a repulsive laser beam along circular trajectories. Center: Increase of temperature as a function of the stirring velocity. For velocities below 1 mm/s, no dissipation is observed as expected for a superfluid system. Right: Evolution of the critical velocity as a function of the local reduced chemical potential ($\mu_{\rm loc}(\mathbf{r})/k_BT$) which depends on the cloud temperature, density and the stirring radius. A sudden jump is observed around 0.22. For lower values, the stirring radius is such that the defect moves in the thermal region. For higher values, the defect moves in the superfluid inner core of the cloud. (From Ref. [73])*

gas by moving a defect created by a repulsive laser beam and measuring the subsequent heating of the cloud. This method had been used previously in 3D Bose gases [74], in Fermi gases [75, 76] and also in dipolar gases [77] to probe their superfluid behavior in a similar way.

In this work, we used a harmonically trapped Bose-Einstein condensate and stirred it with a repulsive laser beam moving along a circular trajectory around the trap center (see Fig. 1.2). We observed that the behavior of the system strongly depends on the radius of the stirrer trajectory. When stirring the inner part of the cloud we observed a critical velocity below which no dissipation occurred. For larger radii we observed no evidence of a critical velocity. We explained this behavior, within a local density approximation picture, by noting that the local degeneracy of the cloud decreases when going away from the center of the trap. The inner region of the cloud is thus superfluid whereas the outer region is in a normal state. The measured critical radius at which the dissipation-less behavior disappears is close to the expectation from local density approximation but we observed that it was systematically higher. This shift could be explained by the finite extension of the stirring laser spot and the fact that the stirring beam should be fully in the superfluid region to avoid dissipation. A detailed numerical modelling of our experiment was recently reported in Ref. [78] confirming our experimental findings. Interestingly, these simulations also revealed two important features. (i) The mechanism underlying the dissipation is the formation of vortex-antivortex pairs, which were not detectable with our experimental setup. (ii) The shift in the determination of the critical radius for stirring can also be explained by the absence of thermalization between the superfluid inner core and the thermal outer cloud. As we were determining the temperature of the cloud from a fit of the thermal wings, this led to a systematic shift in the determination of the amount of dissipation. A recent experimental study in a similar settings of scissor modes, whose presence is linked to the superfluid behavior of the gas, led to similar observations [79].

1.4.2 Emergence of coherence in a 2D Bose gas

This study is published in Ref. [16].

In standard textbooks introducing Bose-Einstein condensation it is usually assumed, whatever is the dimension of the system, that the cloud is essentially isotropic. However, if one considers the cooling of very anisotropic clouds, like pancake-shaped or cigar-shaped systems, the usual criterion for 3D Bose-

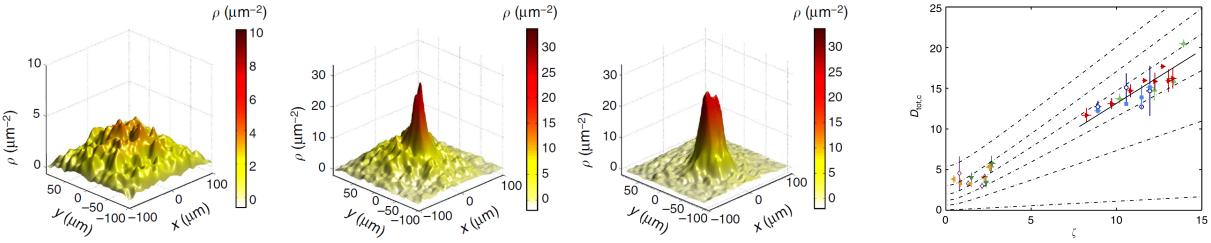

Figure 1.3: *Left: Momentum distribution determined after time-of-flight expansion. From left to right the degeneracy of the cloud is increased and the emergence of in-plane coherence appears as the formation of a narrow peak in the momentum distribution. Right: Critical phase-space density $\mathcal{D}_c$ for the emergence of in-plane coherence. For strong vertical confinement (low ζ) coherence appears for $\mathcal{D}_c$ around 4. For moderate vertical confinement (higher ζ) the critical phase space density increases linearly as expected for a transverse condensation scenario. (From Ref. [16])*

Einstein condensation is not sufficient to fully describe the cooling process. Such a discussion was first introduced in Ref. [80] under the name "two-step" or "transverse" condensation phenomenon. Transverse condensation from a 3D elongated harmonically-trapped cloud to 1D system was experimentally studied in Refs. [81, 82].

The main picture of transverse condensation is that for a trap which is anisotropic enough, Bose-Einstein condensation will develop in two steps when cooling the system. First, the system condenses along the strongly confining direction(s) and, second, full coherence in the weakly confining direction(s) is obtained. In Ref. [16], we have studied the emergence of coherence in a cloud strongly confined in the vertical direction with an approximate harmonic potential (with pulsation ω_z) and confined in plane by a box potential. The in-plane coherence was determined by measuring the momentum distribution of the cloud. It is crucial to realize this study with uniform in-plane confinement to be able to discuss the emergence of long-range coherence without suffering from an inhomogeneous density distribution that could wash out the effects we wish to study.

More quantitatively, we parametrized the problem with the quantity $\zeta = k_B T/(\hbar\omega_z)$. If $\zeta \lesssim 1$, only the ground state along z is populated and the results for a 2D system apply. A richer situation appears for $\zeta \gg 1$. In that case, the threshold for transverse Bose-Einstein condensation in the case of an ideal gas, *i.e.*, the macroscopic accumulation of atoms in the motional ground state along the z direction, is reached when the phase-space density of the cloud reaches $\mathcal{D} = \frac{\pi^2}{6}\zeta$. This value could be much higher than the critical phase-space density for the BKT transition for a perfectly 2D system of interacting particles (~ 8 in our settings) (see Fig. 1.3). We have shown in Ref. [16] that in this case, at the threshold for transverse condensation, the cloud exhibits an in-plane coherence characterized by a decay length on the order of the vertical harmonic oscillator length $\ell_z = \sqrt{\hbar/(m\omega_z)}$ and rapidly increases for lower temperature. It means that in this scenario coherence appears first because of statistics and not because of the BKT mechanism. This value of the coherence length, which increases rapidly for lower temperatures (typically 500 nm in our work) should be compared to (i) the size of the box ($\sim 20\,\mu$m) and (ii) to the thermal wavelength ($\lambda_T \approx 400$ nm). At the transverse condensation threshold we thus observe the onset of in-plane coherence because the correlation length gets larger than the thermal wavelength but this coherence is not extended to the full size of the cloud.

1.4.3 Formation of topological defects in a quenched-cooled 2D Bose gas

This study is published in Ref. [16].

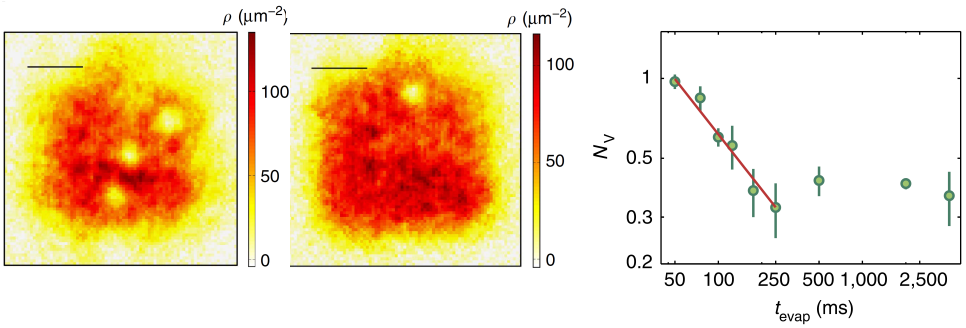

Figure 1.4: *Kibble-Zurek mechanism in a bulk 2D Bose gas. Left: Two examples of pictures of atomic clouds after quench cooling and relaxation. After a short time-of-flight we observe the presence of vortices. Right: Evolution of the number of vortices N_v as a function of the cooling speed. (From [16])*

Quantum gases offer unique perspectives for exploring out-of-equilibrium physics. The understanding of such physics is an extremely vast issue which is still in its infancy. One possible approach to out-of-equilibrium dynamics and more specifically relaxation is based on the Kibble-Zurek mechanism (KZM). This mechanism, first developed in the context of cosmology by Kibble [83] and then applied to second order phase transitions in condensed matter, describes the non-adiabatic crossing of a phase transition and the subsequent formation of topological defects [84].

Consider Bose-Einstein condensation and, starting from the normal phase, a rapid cooling of the system through this phase transition. As the thermalization time diverges around the transition, different parts of the system which are spatially separated will not be able to communicate with each other for a fast enough cooling ramp. Consequently, these different parts will condense independently, each of them with a given value of the phase for the macroscopic wavefunction describing each parts of the cloud. Around the transition point the system is thus frozen in a set of domains with independent phases. The typical size of each domain is given by the cooling speed of the system. This situation corresponds to a strongly out-of-equilibrium configuration that will relax slowly to a state where phase variations are smoothened. However, depending on the phase arrangement of the different domains, a bulk system could relax in a state with topological defects, like point-like vortices in a superfluid.

Kibble-Zurek mechanism has been probed in a large range of systems (see Ref. [85] for a recent review) from atomic physics to solid-state systems. In cold atomic systems, the formation of soliton-like defects when quenching an elongated and harmonically-trapped Bose gas was observed in Ref. [86]. The system being inhomogeneous it allows one to investigate the so-called inhomogeneous-KZM, which shows specific features [87]. KZM has also been studied experimentally for a uniform 3D Bose gas [17, 88], in which the scaling of the correlation length with the cooling time has been measured and critical exponents determined.

In Ref. [16], we described experiments where we performed such a quench cooling on a 2D Bose gas. We observed the formation of vortices, whose density increases for faster cooling ramps (see Fig. 1.4). Indeed, for a faster ramp, more domains are formed and it is then more likely to generate several vortices in the system. A key feature of KZM is the prediction of scaling laws for the evolution of the density of vortices as a function of the cooling speed and the fact that the power-law exponent of this scaling is directly linked to a combination of critical exponents describing the properties of the phase transition, namely the correlation length critical exponent, and the thermalization time critical exponent. In our work, we extract a value for this combination of critical exponents which is compatible with the one expected for Bose-Einstein condensation but this comparison should be taken with care. First, as discussed

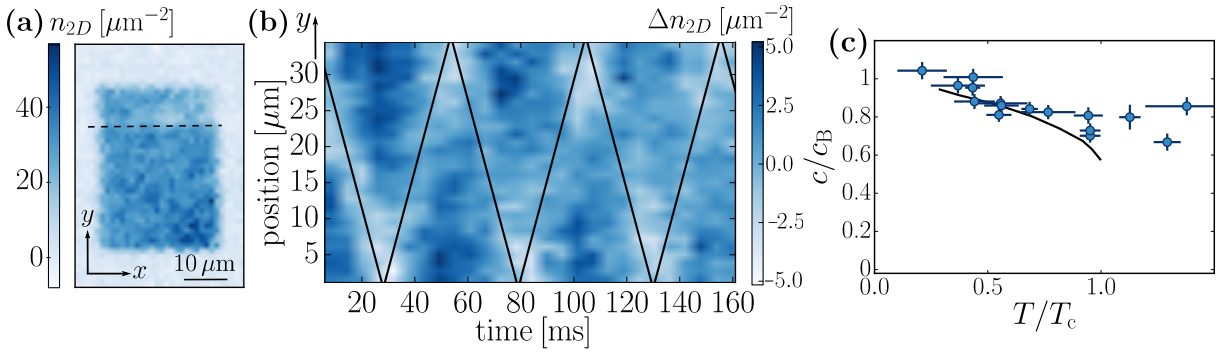

Figure 1.5: *Measurement of the speed of sound in a 2D uniform Bose gas. (a) We excite a sound wave by creating a density perturbation in a rectangular box potential. (b) A density perturbation propagates along the y axis as shown from the time evolution of the x-integrated density profile. Speed of sound is determined for different degeneracies of the gas. Below T_c our measurements are in good agreement with the hydrodynamic prediction (solid line). We also observe sound propagation above T_c that we attribute to a collisionless sound mode.*

in the previous section, during the quench the system evolves from a 3D normal gas to a 2D superfluid and the phase transition we are crossing is more transverse condensation rather than 3D Bose-Einstein condensation. Second, an accurate determination of critical exponents relies on a good understanding of the evolution of the vortices during the relaxation period. Indeed, even if topologically protected, the vortices could move, interact with each other and possibly annihilate, or reach the boundary of the sample and disappear. If this dynamics depends on the quench rate it could alter the investigated scaling law. We will see below that the ring geometry is more robust against this kind of limitations.

1.4.4 Propagation of sound in a 2D Bose gas

This study is published in Ref. [89].

The equation of state of the weakly interacting two-dimensional Bose gas is well-known both experimentally and theoretically [60, 64] and can now be used as a tool to determine experimentally the cloud thermodynamical properties [72, 89]. A challenge for the quantum gas community is still to measure the superfluid fraction of a 2D Bose gas. It has already been measured in liquid helium films but suitable tools are missing for quantum gases. Note that in 3D weakly interacting BECs, superfluid and condensed fraction are almost equal and the measurement of the condensed fraction is routinely realized. An interesting tool to probe quantum fluid is the measurement of the speed of sound. Indeed, in liquid helium two main sound modes are possible, first and second sounds, because of the interplay of the normal and superfluid components as described by the two-fluid model [90].

In a recent theoretical work, propagation of sound in a 2D Bose gas was considered within the hydrodynamic two-fluid model and it predicted the existence of two sound modes as in liquid helium [91, 92]. In a weakly interacting system, the second sound corresponds mainly to a motion of the superfluid part and thus give information about the superfluid fraction. Interestingly, in the limit of very weakly interacting system the speed of second sound squared is directly proportional to the superfluid density [92]. The measurement of speed of second sound thus provides a very interesting way, even if not fully direct in general, to determine the superfluid fraction. To illustrate this link between the superfluid fraction and the speed of second sound, it has been shown in Ref. [91] that the jump of the superfluid transition at the critical point leads to a similar jump of the speed of second sound.

In the work described in Ref. [89] we have excited sound waves (both propagating and standing

waves) with a density perturbation to determine the speed of sound in a range of temperature starting as close as we can from zero to above the critical point (see Fig. 1.5). Our measurements are in good agreement with the prediction of Ref. [91] below the critical temperature. However, above the critical point, we still observed propagation of a density perturbation in contrast to the prediction. This observation could be attributed to a collisionless sound mode [93, 94]. In addition to the speed of sound measurements we also studied the damping of the sound waves. We found a fast variation of damping with temperature compatible with Landau damping prediction [95]. Indeed, Landau damping describes the decay of phonon modes because of collisions with thermal excitations whose population depends obviously on the temperature of the cloud.

Related measurements have been performed previously in 3D Bose gases [96, 97] and Fermi gases [98, 99] but second sound in a 2D quantum fluid had never been observed previously.

1.5 Superfluid currents in a ring geometry

1.5.1 Creation, detection and investigation of superfluid currents

The ability to create custom-shaped potentials on a 2D cloud allows us to explore a wide range of geometries. The ring configuration is of particular interest thanks to its non-trivial topology (which is not simply connected). Because the phase of the wavefunction ϕ of the cloud must be single-valued then the circulation Γ_c of the velocity field $\mathbf{v} = \frac{\hbar}{m}\nabla\phi$ of the quantum gas should follow the quantization condition

$$\Gamma_c = \oint \mathbf{v}.\mathbf{dl} = q\frac{h}{m}, \tag{1.4}$$

where $q \in \mathbb{Z}$. This quantization of the circulation of the velocity field is associated with the existence of quantized superfluid currents along the ring of charge q. The sign of q corresponds to the direction of the rotation of the current and $|q|$ to the amplitude of the current. Equivalently these superfluid currents correspond to vortices whose center coincides with the center of the ring (where no atoms are present).

These superfluid currents are topologically protected because of the quantization condition (1.4). They can only decay by loosing a quantum of circulation. These topological protection has been for instance evidenced in Ref. [100] where we observed that the lifetime of 2D superfluid currents can reach several tens of seconds and is longer than the atomic lifetime. The influence of temperature on the lifetime of superfluid currents is discussed in Ref. [101].

Several experiments studying superfluid currents have been realized. Superfluid currents can be generated deterministically thanks to angular momentum transfer from a pair of Raman beams (in a Laguerre-Gauss mode) [102, 103], and charges up to $q = 10$ have been realized [104]. Another way to create superfluid currents in a deterministic way consists in rotating a barrier along the ring. Indeed, below a critical velocity the motion of the barrier is dissipation-less because of the superfluid nature of the system but, above this critical velocity phase slips, and hence superfluid currents can be created [105, 106]. In our team, we focused on stochastic generation of superfluid currents and we discuss this point below.

The detection of the presence of a superfluid current in a ring is not straightforward because there is no signature of this current on the density distribution. One should thus rely on a measurement of the velocity field, or the phase distribution along the ring. A signature of the superfluid current on the velocity field can be observed in a time-of-flight experiment. When no circulation is present, the initial region with no atoms at the center of the ring gets filled because of the hydrodynamic expansion of the atomic cloud. However, for an initial cloud with non-zero circulation, a hole is visible in the momentum

distribution and its size allows one to determine the amplitude (but not the sign) of the superfluid current [102, 107]. An interferometric method using two internal states have also been developed in Ref. [104] to determine the amplitude superfluid currents. In our team [15, 100], and also simultaneously at NIST [108], we have developed an interferometric method based on matter-wave interference to detect both the sign and the amplitude of the superfluid current. In addition to the ring we want to characterize, we use another cloud, either disk- or ring-shaped, where no circulation is present. After expansion the two clouds interfere and the shape of the interference pattern allows us to determine if there was no circulation in the ring (concentric rings interference pattern) or a given circulation (spiral pattern whose number of arms give the superfluid current amplitude and whose orientation gives the orientation of the current). Finally, another method, based on the measurement of the frequency shift created through Doppler effect has been implemented in [109].

The possibility to move one or several optical barriers (or weak link) in a ring trap makes this system suitable for realizing atomtronics devices, which are the analog of electric devices but using atomic systems. In this context, hysteresis behavior have been demonstrated [110], the relationship between the relative phase between the two sides of the weak-link and the current going through the link have been studied [108, 111]. Atomic rings with two moving barriers have also been realized and have pioneered the study of atomic SQUIDs [112, 113]. Finally, all the results discussed above involves only a single spin component of the system, but rich physics can also be explored with spin mixtures in a ring geometry [114].

1.5.2 Stochastic formation of superfluid currents

Superfluid currents in a ring geometry are topologically protected and hence usually long-lived. Still, they are metastable states and the ground state of the system is a superfluid at rest. The ring geometry is interesting to study out-of-equilibrium dynamics because, starting from an out-of-equilibrium condition, the system could relax either to the ground state or to these metastable states (hosting a superfluid current) that can be easily measured in a experiment. In our team we have investigated two such situations. In one set of experiments we have created independent (and identical) "patches" of atoms along the ring, each of them with an independent phase and we have studied the stochastic formation of superfluid currents when merging them [100]. In another set of experiments we have quenched the atomic ring from a normal state to a superfluid state and observed the formation of superfluid currents [15] in agreement with Kibble-Zurek mechanism predictions. We detail below these two experiments.

Merging atomic patches in a ring geometry

This study is published in Ref. [100] and the full text of the article is reproduced in the appendix.

In this work we have created a strongly out-of-equilibrium situation by merging a set of independent clouds arranged in a ring geometry. Each cloud initially has an independent (and stochastic) phase. When merging the clouds we create boundaries with possibly large phase mismatch that are thus associated with a high kinetic energy. The system then must relax to a configuration with a smoother phase profile which could be either the ground state of the system with no circulation or a metastable state with a given circulation. We have shown in our study that we can predict the statistics of the formation of superfluid currents after merging (see Fig. 1.6). This statistics is in agreement with the widely-used "geodesic rule" which gives a simple way to predict the winding around a loop. It is based on the idea that, for energetic reasons, the system will choose the shortest path between two phases.

With our typical optical resolution of about $1\,\mu$m and given the maximal achievable ring radius of about $20\,\mu$m we have been able to create configurations ranging from 1 to 12 independent clouds and

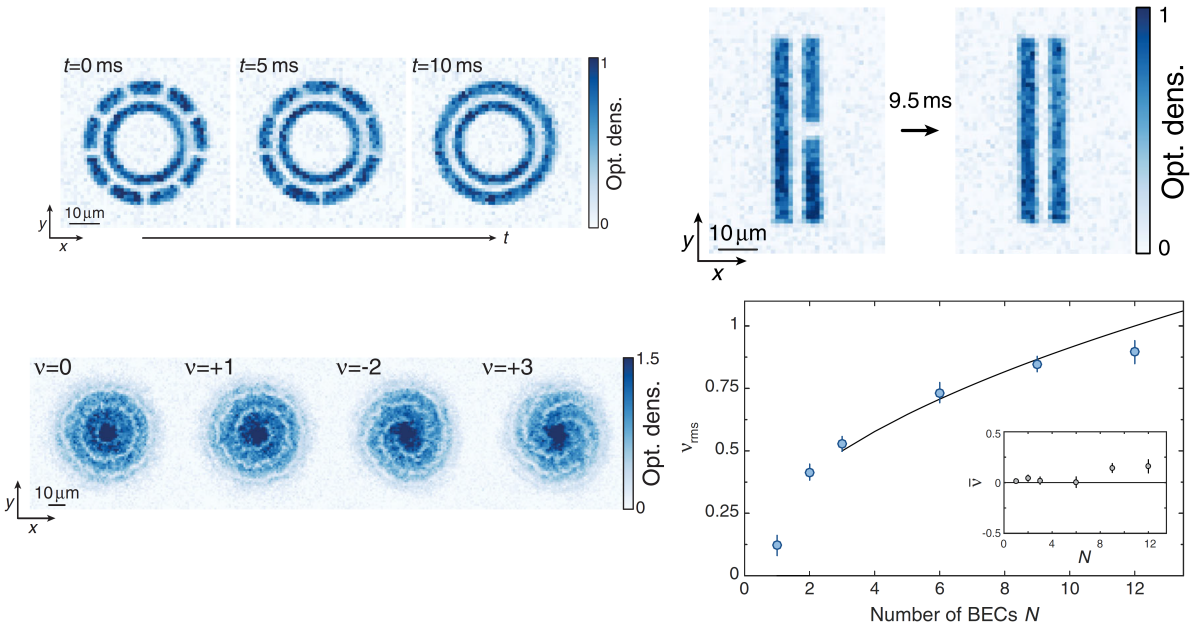

Figure 1.6: *Merging dynamics in box potentials. Top: Merging protocol in a ring geometry and in a two-segment geometry. In both cases, an auxiliary cloud acts as a phase reference for detection. Bottom left: Example of measurements of the phase profile of the outer ring thanks to matter-wave interferences. The orientation and the number of arms of the spiral pattern gives a measurement of the winding number of the superfluid current. Bottom right: Evolution of the width of the distribution of winding number ν_{rms} with the number of segments of the initial ring. The solid line is the geodesic rule prediction. (From [100])*

mostly confirm the geodesic rule prediction. We observed the formation of superfluid currents with the interferometric detection method discussed above which allows us to find both the amplitude and the sign of the superfluid currents. All these measurements were done for a "long" waiting time after merging (0.5 s) to focus only on the formation of supercurrents and not on the more complex short-term dynamics.

In addition, we have explored shorter-term dynamics to unveil the microscopic mechanism at the origin of the smoothening of the phase profile. We observed that the typical time scale for this smoothening is on the order of 100 ms. With our experimental parameters this time corresponds to the time necessary for a perturbation propagating at the speed of sound to make a rotation along the ring. We have been able to monitor the propagation of such phase defects thanks to a complementary experiment. We created a segment of atoms cut in two identical pieces and measured the phase profile of the cloud after merging the two pieces. We observed the time evolution of the phase defect, that can be considered as a gray soliton. This evolution mostly consists in a propagation towards the ends of the segment and a decay of the number of defects on the same time scale as in the ring geometry. We attribute this decay to the fact that the formed gray solitons are unstable in our 2D geometry because of the onset of the so-called "snake instability" [115]. This instability leads to the decay of the soliton into point-like vortices.

A related experiment have been realized with a lattice of Josephson junctions arranged in a ring geometry [116]. In this work the authors used a set of 214 junctions which extend our work, with a very different settings, to large values of the number of patches. They observed, as expected, a normal distribution of values for the circulation but they did not find a quantitative agreement with the geodesic rule.

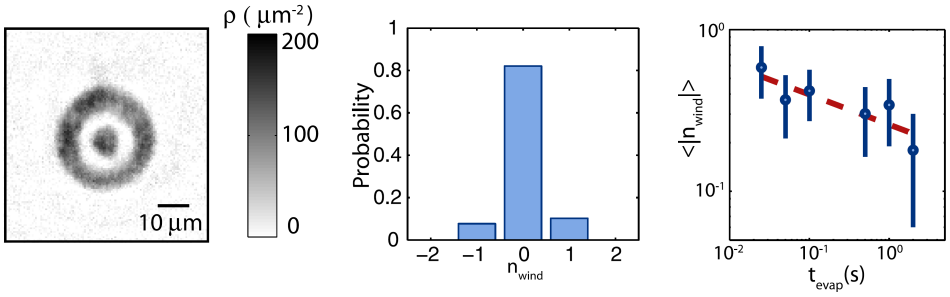

Figure 1.7: *Kibble-Zurek mechanism in a ring geometry. Left: Initial clouds. The inner disk-shaped is the phase reference for matter-wave interferences. Center: Example of probability distribution of the different winding numbers for a cooling time of 2 s. Right: Evolution of the mean absolute winding number* $\langle|n_{\mathrm{wind}}|\rangle$ *with cooling time along with a power-law fit. (From [15])*

Formation of topological defects in a quenched-cooled atomic ring

This study is published in Ref. [15] and the full text of the article is reproduced in the appendix.

As discussed in section 1.4.3, the fast crossing of the critical point when cooling a system through the Bose-Einstein phase transition leads to the formation of domains in the atomic cloud, each of them having an independent and stochastic phase. The relaxation dynamics of this patchwork could lead to the formation of topological defects like point-like vortices in a 2D cloud. In an atomic ring a very similar situation occurs and superfluid currents can be formed [84, 15].

The ring geometry has been put forward by Zurek in Ref. [84] in its gedankenexperiment to apply Kibble's original idea, discussed in the context of cosmology, to solid-state physics and more specifically to liquid helium. This experiment in a ring geometry has never been realized with liquid helium and has only been developed in ring-shaped arrays of Josephson junctions [117]. Our experiment is thus the first investigation of KZM in a superfluid ring. The ring geometry has a major advantage on the bulk configuration. For a narrow enough ring, the typical size of the domains is larger than the width of the ring and the problem becomes one-dimensional. In addition, the formed superfluid currents are much more robust than point-like vortices that can evolve and interact during the quench itself and during the relaxation period. The ring geometry thus offers a better framework for a detailed study of KZM.

A detailed analysis of KZM allows one to extract critical exponents. The determination of critical exponents relies on the model which describes how the different phase domains merge together. In Ref. [84], Zurek determines the link between the number of domains and the distribution of superfluid currents using a 1D random-walk approach for the phase. Assuming that there is a large number of domains N_d which are formed he predicts that the width of the distribution of winding number of the superfluid currents will scale as $\sqrt{N_d}$. The work described in the previous section 1.5.2 is thus of particular importance because it provides and experimental verification of this $\sqrt{N_d}$ scaling. More importantly, it generalizes this scaling to small values of N_d, for which the scaling is not obvious and which corresponds more to our typical experimental situation when investigating quench cooling.

In Ref. [15] we measured the distribution of superfluid currents after quench cooling the gas at different speeds. We observed an increase of the width of this distribution for increasing cooling rate (see Fig. 1.7). From these measurements we deduced an estimate of a combination of critical exponents compatible with the one expected for Bose-Einstein condensation. However, this comparison should be taken with care. Indeed, as discussed above, during the cooling process the system evolves from a 3D normal fluid to a 2D superfluid state and the exact nature of the phase transition we are crossing is not so obvious

to determine.

1.6 Additional works

In addition to the results presented here which focus on the thermodynamical properties of the 2D Bose gas, I have also been working on other themes, related to what have been described above and that I briefly mention in the following.

1.6.1 A proposal to create bosonic fractional Hall states

This study is published in Ref. [118].

Quantum gases are good candidates for exploring quantum-many body systems. An inspiring example is the physics of 2D electron gases submitted to a transverse magnetic field. This system is very rich because of the interplay between the topological band structure experienced by electrons and the presence of interactions which lead to the formation of fractional quantum Hall states whose properties are extremely rich. As we have seen, creating 2D atomic gases is now easily achieved but the orbital effect of a magnetic field is much harder to achieve (see Chapter 4 for a more detailed discussion).

In Ref. [118], we proposed a way to realize fractional quantum Hall states in a small bosonic clouds. The main idea is to use laser beams to transfer angular momentum to the cloud and thus mimic the orbital effect of a magnetic field. We showed that we can adiabatically prepare, for instance, a Laughlin state with a few particles. This method is limited to few particles because of the high value of orbital momentum that should be transferred. However, with current experimental techniques it has now become possible to control the trapping and imaging of a few particles and this protocol could be implemented with typical state-of-the-art methods.

1.6.2 Light scattering in an atomic layer

These studies are published in Ref. [119, 120].

Our experimental setup is well designed to explore the physics of quantum fluids in two dimensions. Interestingly, it is also an original platform to explore basic features of light-matter interactions. Indeed, our atomic cloud can be considered as an ensemble of randomly-positioned scatterers. Atomic scatterers are particularly interesting because they do not allow non-radiative decays which lead to optical absorption like in most solid-state materials. This absorption has been identified as the main limitation for the observation of Anderson localization with light [121]. Moreover, with our typical parameters we are able to explore a regime where the distance between the scatterers becomes smaller than the optical wavelength. In this situation the atomic response becomes collective and leads to a rich many-body problem.

In Ref. [119], we studied the transmission of near-resonant light through a uniform slab of atoms. We observed the presence of a blue shift (on the order of the natural linewidth) of the resonance line. This blue shift has never been observed before and is a striking signature of the collective effects in light scattering. It is for instance opposite to the "textbook" Lorentz-Lorenz red shift which is predicted by classical electrodynamics. Indeed, this mean-field approach does not apply well to a set of fixed scatterers. In addition to this shift, we also observed a large decrease of the optical depth of the cloud and an important broadening of the resonance line.

In Ref. [120], we kept a similar atomic configuration but we locally illuminated the cloud with a laser beam and monitored the in-plane propagation of this optical excitation by monitoring the atomic

fluorescence. We characterized this propagation by a characteristic length and measured it as a function of density of the atomic cloud and detuning of the illumination with respect to the atomic resonance. The most striking feature of our study is the observation of a guiding or anti-guiding effect when changing the detuning from red-detuned to blue-detuned. We attribute this effect to the presence of a transverse gradient of index of refraction whose sign depends accordingly on detuning.

1.7 Conclusion

We have described in this chapter important features of 2D Bose gases and their experimental study. Thanks to the development of several tools, for instance the realization of box-like potentials, we have been able to deepen our understanding of these systems and more generally of the quantum behavior of many-body systems. We have explored different situations including equilibrium properties (coherence), dynamical behavior (superfluidity, sound propagation), and strongly out-of-equilibrium situations (quench cooling, merging of independent clouds). We have also seen that our platform offers an interesting perspectives in the study of light-matter interaction in dense and disordered media. We will describe in the next chapter new projects that could be explored with our current system and with the development of new tools.

CHAPTER 2

Towards 2D uniform Bose mixtures

The studies detailed in the previous chapter focus on 2D Bose gases confined in box-like potentials in a single spin component. A main direction for future experiments is to investigate mixtures of two spin components while still taking advantage of our flexibility in tailoring the shape of 2D uniform Bose gases. In this chapter I describe research plans relevant to this situation. Most of the proposed studies deal with the dynamical behavior of the system probing relaxation dynamics from an initial out-of-equilibrium situation.

When dealing with a mixture it is first important to consider its miscibility. The behavior of the mixtures depends on the relative values of the interspecies interaction parameter $g_{\uparrow\downarrow}$ and of intraspecies ones $g_{\uparrow\uparrow}$ and $g_{\downarrow\downarrow}$, where we have labelled $\uparrow$ and $\downarrow$ the two spin states. Within ^{87}Rb ground state manifold both miscible and immiscible mixtures can be prepared. In the first section of this chapter I will focus on the demixing dynamics that appears when one overlaps two immiscible spin components and present experiments that we plan to realize on this topic. The second section will focus on strongly polarized mixtures and the investigation of impurity physics. In our case the impurity will be made of an atom, say in the spin state $\uparrow$, that interacts with the bath realized by the quantum gas of atoms in spin state $\downarrow$. We will describe how we can specifically address this problem with our system and extend the discussion to the study of a quantum Brownian motion model. Finally, we will also briefly review other interesting perspectives related to our current activities.

2.1 Demixing dynamics

2.1.1 Demixing principle

Demixing dynamics occur when two immiscible fluids are brought together and is a common situation in classical hydrodynamics. For quantum fluids, the situation is very similar and, starting with an out-of-equilibrium mixture of two immiscible fluids, one can observe phase separation between the two components.

The basic features of this demixing dynamics can be well understood by modelling the system by two coupled Gross-Pitaevskii equations describing the two components of the fluid,

$$\left\{ \begin{array}{rcl} i\hbar\dfrac{\partial\psi_\uparrow}{\partial t} & = & -\dfrac{\hbar^2}{2m}\nabla^2\psi_\uparrow + g_{\uparrow\uparrow}n_\uparrow\psi_\uparrow + g_{\uparrow\downarrow}n_\downarrow\psi_\uparrow \\ i\hbar\dfrac{\partial\psi_\downarrow}{\partial t} & = & -\dfrac{\hbar^2}{2m}\nabla^2\psi_\downarrow + g_{\downarrow\downarrow}n_\downarrow\psi_\downarrow + g_{\uparrow\downarrow}n_\uparrow\psi_\downarrow, \end{array} \right. \tag{2.1}$$

where $n_\uparrow = |\psi_\uparrow|^2$ and $n_\downarrow = |\psi_\downarrow|^2$ are the densities in $|\uparrow\rangle$ and $|\downarrow\rangle$. A simple estimate of energy minimization neglecting kinetic energy shows that the miscible or immiscible character is determined by comparing $g_{\uparrow\downarrow}$ to $\sqrt{g_{\uparrow\uparrow}g_{\downarrow\downarrow}}$. Indeed, for $g_{\uparrow\downarrow} < \sqrt{g_{\uparrow\uparrow}g_{\downarrow\downarrow}}$, it costs less energy to mix the two spin components than to separate them and vice versa [122].

In the immiscible case, the equilibrium state at zero temperature corresponds to a full separation of the two components with the creation of two domains. However, situations with more complex interfaces between the two components are energetically close to this ground state and, in the experimental range of temperature, we do not expect to observe full separation but rather a more complex phase separated (and random) situation.

The relaxation dynamics for an initially overlapping mixture is particularly interesting at short times where the emergence of reproducible patterns is expected through a modulational instability [123]. In this situation, some eigen energies of the problem are complex and the modes are unstable. The mode with the largest imaginary part is expected to grow preferentially. The length scale of this mode is typically given by the spin healing length $\xi_s = \xi(g/\Delta g)^{1/2}$, where ξ is the healing length of the gas ($\xi = \hbar/\sqrt{mgn}$). We have introduced g and Δg in a simplify modelling of the system: $g \equiv g_{\uparrow\uparrow} = g_{\downarrow\downarrow}$ and $\Delta g = |g_{\uparrow\downarrow} - g| \ll g$ and we considered equal densities of atoms of the same mass. For $\Delta g \ll g$ the length scale ξ_s becomes large (several microns) and can be easily detected experimentally. The time scale for the emergence of the unstable mode is typically $\tau = \xi_s/c$, where c is the speed of sound in the gas. Demixing dynamics have already been observed in several experiments involving different spin components of the same atomic species [124, 125, 126, 127, 128, 129, 130, 131, 132, 133, 134, 135] or different atomic species [136, 137, 138, 139].

The ^{87}Rb ground state manifold consists in 3 states in the $F = 1$ level and 5 states in the $F = 2$ level. With the usual methods used in our field we can typically create any binary mixtures of the 8 states. These states have different magnetic moments but as we operate in a fully optical trap we are not limited to magnetically trapped states. All the relevant scattering lengths for ^{87}Rb atoms are very close to each other, $a_{\uparrow\downarrow} \approx a_{\uparrow\uparrow} \approx a_{\downarrow\downarrow} \approx 100\,a_0$, where a_0 is the Bohr radius and $g_{ij} = 4\pi a\hbar^2/m$. All mixtures are thus rather close to the miscibility/immiscibility transition and miscible and immiscible pairs are available for ^{87}Rb. For demixing experiments discussed in the following we plan to use the $|F = 1, m = 0\rangle$ to $|F = 2, m = 0\rangle$ transition which has the technical advantage to be insensitive to linear Zeeman effect. For this mixture, following the values given in [140], we have $g_{\uparrow\downarrow}/\sqrt{g_{\uparrow\uparrow}g_{\downarrow\downarrow}} = 1.014$ and it is indeed an immiscible mixture.

2.1.2 Bulk demixing

In a first series of experiments, we will study bulk demixing dynamics. Starting from a degenerate cloud in $|F = 1, m = 0\rangle$ we will apply a short coherent microwave pulse to create a superposition with state $|F = 2, m = 0\rangle$. In this case, the microwave field is homogeneous over the size of the cloud and the mixture will extend all over the cloud. We will then monitor the relaxation dynamics by measuring the time evolution of the *in-situ* density distribution of both spin components.

The main feature of this project compared to previous experiments is our control on the trap geometry. Experiments realized so far were limited to bulk 3D systems or elongated systems along one dimension with the presence of a longitudinal harmonic trap which influenced the dynamics of the spin domains. We will be able to realize similar experiments but without this external harmonic confinement. More importantly, we will also extend the study to 2D uniform systems and will observe the formation of 2D spin domains and their relaxation dynamics. In particular, we will investigate the role of the (hard-wall) boundary conditions on the pattern formation. We will also study the phase evolution of the two-component mixture [131].

Finally, we emphasize that this dynamical formation of patterns is strongly related to the formation of matter wave solitons in attractive single-component BECs [141, 142]. For $g_{\uparrow\downarrow} < g_{\uparrow\uparrow}, g_{\downarrow\downarrow}$, one can show that Eq. (2.1) can be separated as two single-component attractive Gross-Pitaevskii equations (for

a fixed total density) [143, 144, 134].

2.1.3 Demixing at an interface

We also propose to go beyond the bulk situation and investigate the dynamics of the interface between two spin domains. First, we will study the time evolution of the interface when the two components are at rest and in different geometries (see Fig. 2.1). The initial states are expected to be stable at zero temperature but we will investigate the time dynamics of the interface as a function of the temperature of the sample. As the characteristic energy scale of the interface is very low, this technique could be a sensitive probe at very low temperatures where usual methods fail. Second, when a relative flow is imposed between the two components, hydrodynamical instabilities are predicted. A flow perpendicular to the interface is expected to give rise to a Rayleigh-Taylor instability [145, 146] and the growth of mushroom-like pattern is expected. A tangential flow will lead to a Kelvin-Helmholtz instability [147, 148] and the formation of a saw-tooth shaped interface at short time that will decay through the emission of point-like vortices. We also expect capillary instabilities for narrow tubes of one component immersed in the second component [149]. Finally, for a bubble of atoms moving in the other component, the formation of vortices above a critical velocity has been studied in Ref. [150]. This will open the perspective to study superfluid dynamics in a way reminiscent to the study of superfluidity we performed with a stirring laser in [73] replacing the obstacle by (impurity) moving atoms. It deserves to be revisited with smaller obstacles to avoid excitations due to the finite size of the stirring beam which prevent direct observation of the Landau critical velocity. A related study was reported in Ref. [151] but it focused on the scattered atoms and not on the precise dynamics of the impurities.

The investigation of this wealth of dynamical effects in two-component BECs requires a suitable tool-box to create bubbles of impurities with a controlled spatial shape and with a tunable initial velocity. We will realize spatially-resolved spin transfer thanks to two-photon Raman transitions to couple the two spin states and use our good spatial resolution to select the region in the cloud where spin transfer will be realized. To have full control over the shape of this region we will reflect the Raman beams of an additional DMD whose pattern will be imaged on the cloud. The relative momentum between the two components will be imparted by the Raman beams. This momentum transfer ranges from zero, for copropagating Raman beams, to in-plane velocities on the order of the speed of sound for beams crossing at an angle and with taking into account the geometrical constrains in our setup. Interestingly, we can easily extend this study to miscible mixtures or to situations with only a momentum transfer without changing the internal state.

It is important to keep in mind that the previous discussion focuses implicitly on "ideal" binary mixtures with no relaxation. This picture could be modified by spin-changing collisions that for instance will convert a pair of atoms in $|F = 2, m = 0\rangle$ to a pair of atoms in $|F = 2, m = \pm 1\rangle$ as investigated for instance in the seminal experiments reported in Refs. [152, 153, 154, 155]. Hyperfine relaxation can also occur and the $|F = 2, m\rangle$ states are expected to decay into $F = 1$ state. This causes losses owing to the large hyperfine energy splitting.

2.1.4 Possible extensions

Feshbach resonances For the spin components we aim at investigating first ($|F = 1, m = 0\rangle - |F = 2, m = 0\rangle$), the interaction parameters are fixed. It would be interesting to tune these parameters for a more complete investigation of demixing dynamics. The intraspecies interaction parameters cannot be changed easily for ^{87}Rb; however an interspecies Feshbach resonance exists for the $|F = 1, m = -1\rangle$–$|F = 2, m = 1\rangle$ mixture [156] and has been characterized in Ref. [132].

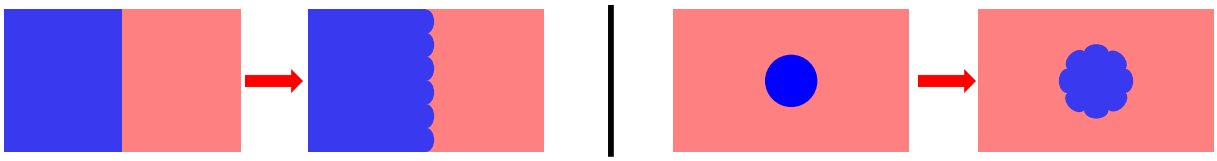

Figure 2.1: *Principle of a demixing experiment. We create an interface between two spin domains and then monitor the formation of patterns at this interface that are expected to appear through a dynamical instabilities. With our apparatus we will be able to realize custom-shaped interfaces like linear (left) or circular (right) ones.*

Rabi-coupled two-component BECs Another interesting degree of freedom is to couple the two components (continuously). This allows to tune the miscibility of the system and to cross dynamically the miscible-immiscible phase transition [157, 158].

Topological defects in binary mixtures Superfluid systems host topological defects like point-like vortices or superfluid currents in ring geometries as discussed in the previous chapter. Multi-component superfluids host a much richer variety of topological defects as systematically investigated in Ref. [28] (see also [159] for a simplified discussion). Example of such defects are coreless vortices like skyrmions, which have been observed in spinor condensates [160, 161, 162]. Half-quantized vortices have also been observed [163, 164] and it has been recently proposed that their dynamics could simulate quark confinement [165, 166].

2.2 Impurity dynamics

2.2.1 Bose polaron

The concept of polaron has been first introduced by Landau and Pekar in condensed-matter physics to describe the motion of an electron in the bath of atoms constituting the solid [167]. The central idea is to introduce a quasiparticle state, the polaron, which describes the dynamics of the electron as a free particle with, among others features, a renormalized mass. The main interest of this situation is to deal with a rich many-problem for which theory can be pushed quite far (see [168] for a review of the Bose polaron case). In the context of quantum information, the study of the dynamics of the impurity in the bath can also be considered as the decoherence of a quantum system because of the interaction with a environment.

This concept has been adapted to the study of impurity dynamics in quantum gases experiments which propose ideal platforms to investigate this problem. The case of fermionic impurities in a Fermi bath is introduced in [169] and experiments are reported for instance in Refs. [170, 171, 172]. Decoherence of fermionic impurities in a Bose gas have also been studied in [173].

The Bose polaron problem is often modelled in a simple approach by the so-called Fröhlich Hamiltonian (see [168] for a discussion on the associated approximations) which captures many features of this problem:

$$H = \frac{\mathbf{p}^2}{2m} + \hbar \int d^3k\, \omega_k\, \hat{a}^\dagger_{\mathbf{k}} \hat{a}_{\mathbf{k}} + \int d^3k\, V_k\, e^{i\mathbf{kr}} (\hat{a}^\dagger_{-\mathbf{k}} + \hat{a}_{\mathbf{k}}). \tag{2.2}$$

The first term describes the kinetic energy of the impurity of mass m, position $\mathbf{r}$ and momentum $\mathbf{p}$. The second term describe the Bogoliubov modes of the boson bath with wavevector $\mathbf{k}$, frequency ω_k and the

corresponding creation operator $\hat{a}_{\mathbf{k}}$. The last term describes the coupling between the impurity and the bath with a matrix element V_k for a mode $\mathbf{k}$ and which is linear in $g_{\uparrow\downarrow}$ and in $\sqrt{n_0\xi^{-3}}$, where n_0 is the condensate density. The matrix element V_k takes important values for modes with $k > \xi^{-1}$ [168]. This Hamiltonian can be derived from a microscopic model [168].

In short, one can distinguish three regimes depending on the interaction strength between the impurity and the bath that we can characterize by the dimensionless ratio $\alpha = g_{\uparrow\downarrow}/[g_{\downarrow\downarrow}(n_0\xi^3)^{-1/2}]$. The low-coupling regime, $\alpha \ll 1$, can be well described in the mean-field approximation. In the strong coupling regime, $\alpha \gg 1$, self-trapping of the impurity is expected. In the (maybe most interesting) intermediate regime the impurity creates effective phonon-phonon interactions.

Several experiment have been realized in lattice geometries (see for instance [174, 175, 176]). We focus here on experiments in bulk systems. The motion of impurities in a 1D gas has been studied [177, 178] and the shift of the energy of the motional states of an impurity because of the bath of phonons has been measured in [179]. The strongly interacting regime (both attractive and repulsive) has been probed via spectroscopy in Refs. [180, 181].

2.2.2 Quantum Brownian motion

We are interested in the study of impurity dynamics in the framework of Quantum Brownian Motion (QMB) (see Fig. 2.2). This model is a paradigmatic example of the physics of an quantum open system. It describes the physics of a particle moving in a bath of non-interacting harmonic oscillators satisfying Bose statistics [182]. This situation is very close to the Fröhlich Hamiltonian of Eq. (2.2) but one needs to assume that $|\mathbf{kr}| \ll 1$, to obtain a coupling of the impurity and the bath linear in position and find the QMB Hamiltonian. It is shown in Ref. [182] that this approximation corresponds to the regime of low temperatures and short observation times. The typical values proposed in this study are challenging to realize (temperature in the 10 nK range) but are still experimentally realistic.

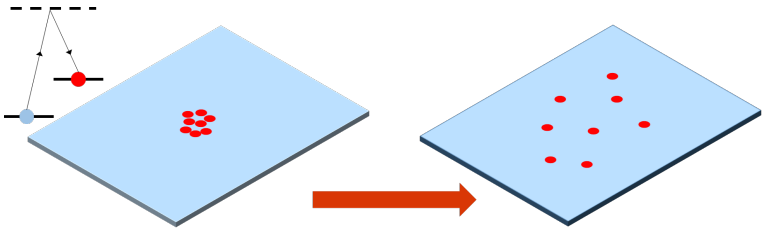

Figure 2.2: *Principle of Quantum Brownian Motion. We study the dynamics of spin impurities (red dots) in a quantum bath (blue) created by a superfluid of atoms in another spin state.*

In the QMB regime, the diffusion of the impurity is expected to be strongly anomalous [182]. It has been shown that the dynamics of the impurity is non-Markovian, *i.e.*, it possesses memory effects. More in detail, the bath is super-ohmic meaning that the impurity has a superdiffusive behaviour.

Many theoretical studies on QMB applied to quantum gases has been proposed [183, 184, 185] but no experiment achieving this regime has been reported yet. The group of A. Widera in Bonn has recently made significant achievements in this direction by studying the motional and spin dynamics of single Cesium atoms in a Rubidium cloud [186, 187, 188, 189]. However, inelastic three-body losses in Cs-Rb collisions appear on the millisecond time scale for typical BEC densities and are an important limitation to the study of the long-term dynamics of the QMB.

Our project is based on an experimental approach where the impurity atoms will be made by another spin component thus limiting inelastic losses. The limitation in this case is that the impurity-bath inter-

action strength will be fixed and very similar to the interaction strength in the bath, thus preventing to explore the strongly interacting regime between the impurities and the bath. In addition, we will implement on our setup the now widely-developed single atom imaging techniques to observe the impurity dynamics [190, 191, 192].

2.3 Other projects

For the sake of concision and coherence we have focused in this chapter on the physics of binary mixtures. However, several interesting studies can also be carried out with single component systems. We briefly review two of them.

First-order correlation function measurement In 2D superfluids we expect that the first-order correlation function, describing phase coherence in the system, decays algebraically with distance. This correlation function can be determined through the Fourier transform of the momentum distribution [44]. It could be also directly measured by interfering two copies of the same gas as recently done in 3D uniform gases [17]. We have already conducted (unpublished) experiments to measure the momentum distribution and we could in addition develop the interference method using the Raman system mentioned previously for creating spatially-resolved binary mixtures. Our experimental system provides us a unique opportunity for this study because it has been shown that algebraic decay is strongly modified in inhomogeneous gaseous systems [193] and in (out-of-equilibrium) polaritonic systems [194, 195]. If successful a natural extension of the work would be to study non-equilibrium dynamics in this system. For instance, the formation of topological defects when crossing the transition *à la* Kibble-Zurek could be studied (even if the BKT transition is not a second-order phase transition) and one could possibly measure the dynamical critical exponent of this transition.

Quantum transport The study of conductance in a two-terminal setup, where a channel is connected to two reservoirs, has been a long standing subject which has recently attracted a growing interest thanks to the emergence of mesoscopic physical systems. Quantum conduction of electrons or phonons through a mesoscopic channel has been widely studied and the observation of the quantization of charge and thermal conductance has been observed in several settings [196, 197]. Clearly, quantum gases experiments open a new window on this rich situation. The intake of cold atoms setups have been exemplified with the recent work of the ETH group at Zurich on Fermi systems [198, 199, 200]. The ETH group has studied thermoelectric effects [201] and the role of disorder on superfluidity for a 2D channel [202]. They also reached the single-mode regime and studied the conductance through a quantum point contact, observing the fermionic quantization of conductance [203] and characterizing spin conductance [204]. More recently, they developed techniques to monitor locally the dynamics in the channel [205] or to study transport in the presence of an additional lattice potential along the channel [206]. They also studied the dynamics of the system beyond ballistic transport (relevant for non-interacting fermions) and observed the dynamics of two resonant Fermi reservoirs coupled through a quantum point contact [207]. These studies have been complemented by a recent work at LENS [208, 209] where Josephson oscillations between two interacting Fermi gases have been studied.

Transport properties with weakly interacting bosons have been discussed in Refs. [210, 211, 212, 213]. However, a single experimental study has been reported so far [214]. In this work the authors determined the conductance of a mesoscopic channel but starting from a (very) far from equilibrium

situation where all the atoms are initially in a single reservoir, a regime where linear response theory do not apply. This study was done for a very degenerate cloud and only particle transport was investigated.

Using our experimental apparatus we will explore particle and heat transport in a channel. We will start with the very degenerate configuration, where the well-known Josephson-like physics occurs and then move to the non-zero temperature regime where the dynamics of the normal and condensed fraction are expected to differ and lead to non-trivial two-fluid dynamics [211]. In this regime we will study the analogue of thermoelectric effects for neutral particles. We will also extend this study to situations where disorder is present in the channel. We will address the possibility to observe the analogue of the celebrated fountain effect, which is a cornerstone of the superfluid character of liquid helium. The application of this effect to Bose gases has been recently discussed in [210].

A key motivation for this project is to extend these studies to narrow channels and more specifically to the regime where only a few discrete modes of conduction are available, thus entering the quantum regime for transport in a situation similar to the celebrated Landauer setup [215]. For electrons, the discretization of the conducting modes leads to the quantization of electric conductance in steps of e^2/h. Fermi statistics is crucial to justify this quantization and the behaviour of bosons is expected to be very different because of their statistics [213]. A plateau of conductance is still expected but its value is much larger and non-universal as it is temperature dependent. The role of interactions for bosons is important and should be considered for a full understanding of this situation. In addition, we will investigate heat flow in a single-mode channel. Heat conductance is expected to be quantized with a universal value $\pi^2 k_B^2 T/3h$ [216] which is independent of the quantum statistics and has never been observed for massive bosons so far. Here again, the role of interactions is still an open theoretical and experimental question.

CHAPTER 3

Ytterbium quantum gases in optical lattices

3.1 Introduction

Most of the experiments with quantum gases are realized with alkali atoms. These atoms have a simple level structure suitable for efficient and simple laser cooling schemes, like the rubidium atom used in the experiments described in chapter 1. This advantage is in balance with the many novel features accessible with more "exotic atoms". Metastable helium, who has an effective level structure similar to alkali give access to unique detection possibilities through electronic detectors [217, 82]. Chromium, dysprosium and erbium, which have been Bose condensed, have a very high magnetic moment and are suitable for studying gases with long-range dipolar interactions [218, 219, 220, 221]. Two-electrons atoms like alkaline-earth (strontium and calcium) or the lanthanide ytterbium have an interesting very long-lived (in the few seconds range) electronic metastable state that is weakly coupled to the ground state by an optical transition. These atoms have been Bose condensed in several groups [222, 223, 224, 225, 226, 227].

This metastable state and the associated ultranarrow transition are useful for several reasons. The most important application is for the design of optical atomic clocks [228]. The idea in that case is to stabilize the frequency of a narrow linewidth laser to the atomic resonance and to use this laser as a frequency standard. Second, thanks to the narrow linewidth, one can realize optical coherent control with negligible spontaneous emission which can be used for quantum information processing [229]. Dealing with an optical transition, it is possible to control coherently the motional degrees of freedom, for instance to implement spin-orbit coupled systems [230, 231]. We will see below in this chapter that such coherent coupling on a clock transition is also the cornerstone of the proposal that we plan to implement to create artificial magnetism [34].

Ytterbium atoms (and similarly strontium atoms) have several stable isotopes, both bosonic and fermionic. The ground state of ytterbium atoms is a spin-singlet $^1S_0$ state. Bosons have zero nuclear spin and the ground state is thus non degenerate. Fermions have a non-zero nuclear spin. The two stable isotopes, ^{171}Yb and ^{173}Yb have an hyperfine spin $1/2$ and $5/2$, respectively. In both case the ground state is thus a degenerate manifold with $N = 2, 6$ states associated with a SU(N) symmetry. These features have been explored in ytterbium experiments in Refs. [232, 233, 234]. In this manuscript, we report studies realized on bosonic ^{174}Yb.

In the first part of this chapter, I describe the development of the ytterbium experiment and the results obtained so far. In the last section I present our research plans towards the realization of artificial magnetic fields on a lattice system.

3.2 A new experiment

A large part of these results are discussed in more details in the two PhD theses [235, 236] written by the students who started the ytterbium experiment. Three PhD students are currently working on the setup, M. Bosch, R. Bouganne, and A. Ghermaoui. Two postdoctoral fellows, D. Döring and Q. Beaufils also contributed to this work. This project is conducted in collaboration with F. Gerbier.

3.2.1 Bose-Einstein condensation of ^{174}Yb

Atomic levels and cooling lasers

Here we focus on ^{174}Yb which is the most abundant boson. We report in Fig. 3.1 the lowest-lying and relevant levels of ytterbium atoms. We will mainly use in the following four transitions:

- The broad $^1S_0 \rightarrow ^1P_1$ "blue" transition at 399 nm which offers a large scattering rate for laser cooling but which is not a completely closed transition. ($\Gamma/2\pi \approx 30$ MHz)
- The narrow $^1S_0 \rightarrow ^3P_1$ "green" transition at 556 nm for which the associated Doppler temperature is as low as 4 μK. ($\Gamma/2\pi \approx 0.2$ MHz)
- The ultranarrow $^1S_0 \rightarrow ^3P_0$ transition at 578 nm. ($\Gamma/2\pi \ll 1$ Hz)
- The repumping transition $^3P_0 \rightarrow ^3D_1$ to measure the population in the metastable state. ($\Gamma/2\pi \approx 0.4$ MHz)

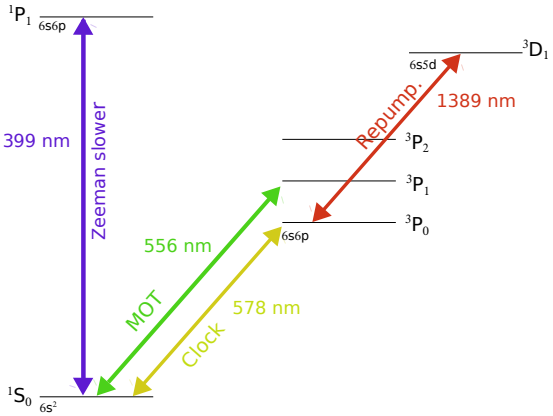

Figure 3.1: *Low-lying states of bosonic ytterbium atoms*

Experimental design

The design of the setup was largely inspired by the one of the Kyoto team [225]. An atomic beam is Zeeman-slowed using a laser resonant on the "blue" transition and loaded into a magneto-optical trap (MOT) operating on the "green" transition. Atoms are then loaded in an optical dipole trap and transported to a science chamber with a large optical access. After evaporative cooling, an almost pure BEC is formed with about 6×10^4 atoms. This BEC is the starting point of all experiments.

When inducing transitions to the metastable state, it is useful to transfer the atoms in optical traps operating at the magic wavelength. For this specific wavelength (~ 760 nm for Yb) the trapping potential is the same for the ground and the metastable state so that there is no differential lightshift between the two states. For the experiments described in the rest of this chapter, the BEC is either transferred in another dipole trap or in 3D optical lattices, all operating at the magic wavelength.

3.2.2 Ultranarrow linewidth laser

Driving the clock transition requires a laser with a well-defined and stable frequency. More precisely, we will consider the linewidth of the laser defined on a short duration corresponding to typical durations of the light pulses we will shine on the atoms ($\sim 1 - -100$ ms). In addition, the central frequency of the laser should remain stable during many experimental runs, meaning at least several minutes. These two

features should be compared to the relevant experimental frequency scale which is mostly given by the Rabi frequency Ω of the excitation that is around 1 kHz in our case. Our typical requirements are then:

- The linewidth should remain small compared to Ω, corresponding to a few tens of Hz
- The variation of the central frequency over several minutes should also be small compared to Ω.

Note that slow and deterministic drifts can be compensated by calibration runs whereas random fluctuations are more detrimental. These requirements are challenging to fulfil and we have used techniques developed by the optical clock community to achieve them.

Laser design

To obtain a laser at 578 nm, we use sum frequency generation. The two pump sources are commercial narrow-linewidth lasers: a fiber laser at 1030 nm and a YAG laser at 1319 nm with linewidths in the several kHz range. We use a single-pass bulk crystal for the non-linear conversion , obtaining typically a few tens of mW.

Frequency stabilization

Even if commercial lasers are already quite narrow, they are far from the required linewidth. The idea developed for atomic clocks is thus to frequency lock the laser on a high finesse cavity. We use a commercial cavity consisting of two mirrors contacted on a ultralow expansion (ULE) glass spacer. This cavity is placed inside a thermal shield and under vacuum to minimize its length variations. The cavity length is about 50 mm. The linewidth of the reflection peak of the cavity is about 10 kHz and we frequency lock the laser on the peak. It is thus important to optimize the electronic feedback loop so as to lock with an accuracy 100–1000 times smaller than the linewidth. Measuring the amplitude of the error signal of the lock we estimate that the laser linewidth should be below 100 Hz.

Absolute frequency determination

With the method described above, the laser frequency is fixed by the cavity. But the absolute value of the resonance of the cavity is *a priori* not known accurately and is drifting with time. We found it convenient to use molecular iodine to determine the frequency of the laser and tune it close to the correct value. We developed a saturated absorption spectroscopy to measure the absolute laser frequency with an accuracy of about 20 kHz [236]. This greatly facilitated the finding of the Yb resonance. Today, the typical cavity drift is around 4 kHz per day. This drift is typical for such cavities and can be attributed to slow relaxation of the materials used to fix the cavity length.

3.3 Probing quantum gases on an optical transition

3.3.1 Introduction

Bose-Einstein condensates are often detected by measuring their momentum distribution obtained after release and expansion of the trapped clouds and using absorption imaging, like in the seminal works in 1995 [5, 6]. However, the first BEC of hydrogen atoms was detected by spectroscopy on an optical transition [237]. Indeed, probing a system on a narrow optical transition allows to probe small frequency shifts like, for instance the one due to interactions between particle. It is also possible to obtain information on the momentum distribution of the cloud by measuring frequency shifts due to Doppler effect.

Spectroscopy measurements on an optical clock transition is thus a very useful tool for characterizing properties of quantum gases. This tool has many common features with standard techniques in our community to induce transitions between hyperfine ground states, like microwave spectroscopy or two-photon Bragg/Raman spectroscopy.

The work described in this section illustrates this through several examples. First, we show measurements of momentum distributions thanks to Doppler spectroscopy in an untrapped and expanding cloud. Second, we detail optical spectroscopy of few atoms confined at the sites of an optical lattice operating at the magic wavelength. These measurements allowed us to determine the so far unknown collisional parameters of ground and metastable atoms. Third, we investigate spectroscopy of a BEC trapped in a magic dipole trap. All these studies also allowed us to develop and characterized our clock laser system.

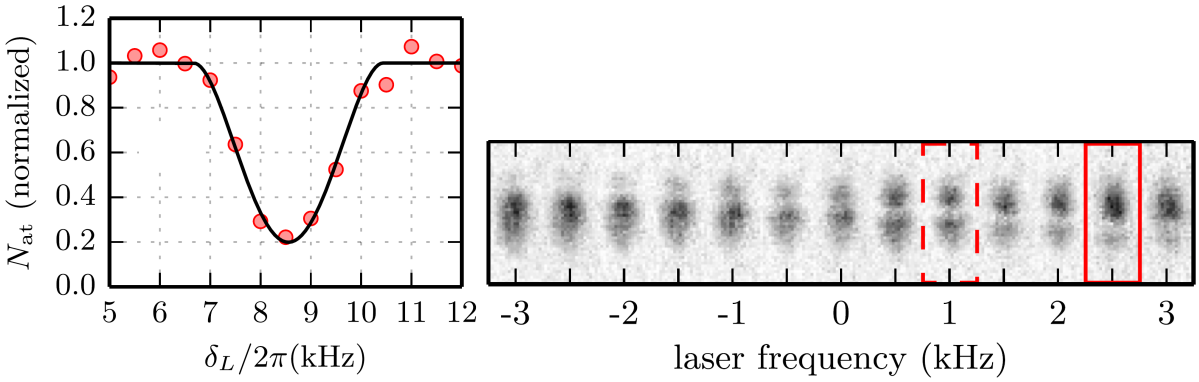

Figure 3.2: *Left: Spectroscopy of a cloud during time-of-flight. The linewidth of the line mostly reflects the velocity distribution of the cloud through Doppler effect. Right: Imaging of the laser frequency. We first let the cloud elongate into a 1D waveguide to obtain a large velocity distribution. We then probe the cloud with the clock laser and observe a dip in the absorption signal of the ground state atoms corresponding to a slice of atoms resonant with the clock laser. The position of the slice in the guide gives access to the absolute frequency of the laser. The width of the slice may be used to determine the linewidth of the laser in a single-shot measurement. A similar technique in position space has been recently reported in Ref. [238]. (From Ref. [236])*

3.3.2 Doppler spectroscopy

This study is published in Ref. [236].

For these experiments, the BEC was confined in a dipole trap realized by a combination of two lasers (at 532 and 1070 nm) which were not at the magic wavelength. The lines measured by *in-situ* spectroscopy are thus dominated by differential lightshifts effects that we are not interested in. For these first spectroscopic experiments we realized a measurement after a time-of-flight of the BEC to remove this kind of frequency shifts. For a long enough time-of-flight the initial interaction energy between particles is entirely converted into kinetic energy. Spectroscopy allows us to measure the velocity distribution via Doppler effect (see Fig. 3.2). With our parameters we measured linewidths about 1-2 kHz, which are limited by the width of the velocity distribution and not the laser linewidth. In addition, by controlling the expansion of the cloud in a 1D "tube", we observed that the resonance becomes spatially dependent. Indeed, after expansion, each position in the cloud corresponds to a given class of velocity. If the laser linewidth is smaller than the corresponding range of velocities, then only atoms in the resonant velocity class are transferred to the metastable state (see Fig. 3.2). This technique gives a measurement of the

laser frequency in a single-shot and could be used to efficiently compensate for the slow term drifts of the laser frequency or to determine the laser linewidth (defined on the duration of a single experiment).

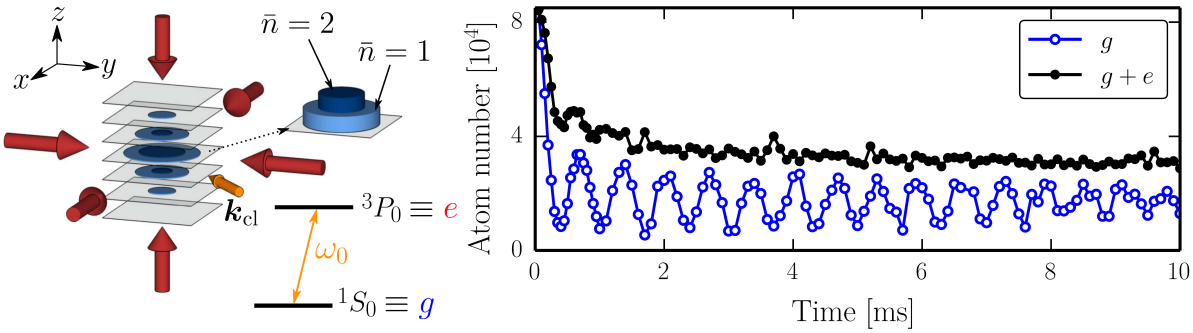

Figure 3.3: *Clock spectroscopy in a deep optical lattice. Left: experimental scheme. We create a stack of 2D optical lattices containing typically 1 or 2 atoms per site in the Mott insulator regime and probe them with the clock laser. Right: Time evolution of the ground state population and the total population. After 1 ms we observe weakly-damped Rabi oscillations demonstrating the coherent control of the clock transition. This regime occurs after a fast decay of the total atom number during the first period of the Rabi oscillation. We attribute this decay to inelastic losses between excited state atoms in doubly-occupied sites. The subsequent oscillations thus correspond to the dynamics of singly-occupied sites. (From Ref. [239])*

3.3.3 Spectroscopy of a Mott-Insulator

This study is published in Ref. [239].

In this work, we prepare an ensemble of independent 2D clouds each confined at a different site of the vertical optical lattice. The in-plane square lattice is tuned to a depth around 25 $E_{\rm r}$, where $E_{\rm r}$ is the recoil energy. This depth is large enough to allow one to consider that the sites of this lattice are isolated on the time-scale of our spectroscopy experiments.

We coherently couple the two states and observed first a fast decay and then long-lived Rabi oscillations (see Fig. 3.3). At short times some sites contains two atoms (or more) and we attributed this rapid decay to inelastic losses between atoms in the metastable state at a rate $\beta_{ee} \approx 3 \times 10^{-11}\,\mathrm{cm^3 s^{-1}}$. We have also shown that the ground-metastable inelastic collision rate is negligible on our experimental time scales. After the first millisecond, the Rabi oscillations correspond to the coherent driving of isolated atoms in singly-occupied sites.

In a second set of experiments (not shown here), we determined the interaction parameters by spectroscopy. When two atoms are present at a single site one should consider the two possible transitions $|gg\rangle \rightarrow |eg^+\rangle = (|eg\rangle + |ge\rangle)/\sqrt{2}$ and $|eg^+\rangle \rightarrow |ee\rangle$. When there is no interaction between the two particles, these two transitions are degenerate but otherwise they are respectively frequency shifted by $U_{eg}/\hbar$ and $(U_{ee} - U_{eg})/\hbar$, where U_{ij} are the on-site interaction energy between two particles in states i and j in the Bose-Hubbard model [239]. Measuring these frequency shifts allows one to determine the interaction shifts and then, with a proper calibration of the confinement in each site, the corresponding scattering length a_{eg} and a_{ee} (from the known value of a_{gg} [240]). We obtained $a_{eg} \approx a_{ee} \approx a_{gg} \approx 100\,\mathrm{a_0}$, meaning that all transitions occur at very similar frequencies. With our experimental parameters, this corresponds to frequency shifts on the order of 100 Hz. Similar experiments have been realized concomitantly at LENS in Florence and report compatible values [241]. More recently, a related study has been performed on strontium atoms with a 10-spin component fermionic cloud [242].

Spectroscopy in deep optical lattices also allowed us to estimate the clock laser linewidth. We measured shot-to-shot fluctuations with a standard deviation of about 100 Hz. This values is close to our expectations but remains a bit large and could be a limitation for us in future works. In a recent set of measurement we have shown that these fluctuations do not correspond to the laser linewidth but to fluctuations of the central frequency from one experimental run to the other. These fluctuations may be attributed either to phase noise during propagation of the clock laser from the cavity to the atoms seems or to uncontrolled fluctuations of the cavity frequency.

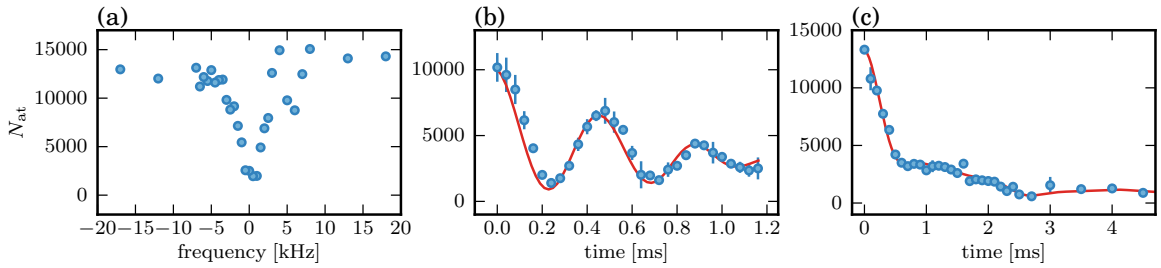

Figure 3.4: *Spectroscopy of a BEC in a 3D magic dipole trap. Left: In-situ excitation spectrum of the BEC. The typical width of line reflects the dispersion of interaction energy for the non-uniform intensity distribution. Middle and Right: Two examples of Rabi-like oscillations. We observe damped oscillations or non-linear relaxation. The Rabi frequencies are $\Omega/2\pi$ =2.1 and 0.8 kHz and the chemical potential is given by $\mu/h \approx 1$ kHz for both curves.*

3.3.4 Spectroscopy in a magic dipole trap

This study is published in Ref. [243].

The experiments in a deep optical lattice described above probe the laser excitation of few particles. This well-controlled situation allowed us to determine accurately the relevant collisional parameters of ytterbium atoms. We now consider the excitation of an *in situ* BEC confined in a magic dipole trap, where no differential lightshifts are present. In this situation clock spectroscopy mainly gives information about the interaction energy between particles (on the order of a few kHz) and to a lesser extent about the Doppler broadening due to the non-zero size of the trapped BEC ($\sim v_r/R \sim$ few hundreds Hz, where v_r is the recoil velocity and R the typical size of the BEC) (see Fig. 3.4a). Optical spectroscopy on narrow transitions has also been reported in Refs. [244, 245, 246] and the role of interactions and quantum statistics has been studied. However, coherent driving has not been explored yet.

We show in Fig. 3.4b-c two examples of Rabi-like oscillations at two different clock laser intensities. For large Rabi frequencies, we observe damped oscillations whose damping can be attributed to a combination of dephasing, due to elastic interactions in the cloud and inhomogeneous Doppler broadening, and to losses due to inelastic collisions in the metastable state. For small Rabi frequencies, the behaviour is more complex and involves the role of momentum transfer by the clock laser, density redistribution in the cloud, etc. We describe well the behavior in all regimes thanks to a two-mode dissipative Gross-Pitaevskii model including the values of the collisional parameters determined in [239] (see the red solid lines in Fig. 3.4). The observed dynamics, from damped oscillations to a monotonic decay, is a good example of the time evolution of an assembly of two-level systems undergoing relaxation by coupling to the environment. In our experiments, decoherence is due to different dephasing mechanisms and losses and, depending an the strength of the driving with respect to these mechanisms, we observe an evolution from an oscillating weakly-damped regime to an overdamped regime where an irreversible decay is

observed.

3.4 Towards topological phases in optical lattices

3.4.1 Motivation

The main motivation for the building of the ytterbium experiment is to study strongly correlated quantum phases of matter in topological band structures. This topic is inspired from the rich physics emerging for 2D electrons gases submitted to a strong transverse magnetic field, in particular the case of quantum Hall physics [50]. The main feature of the integer quantum Hall effect is the quantization of the transverse conductance of a 2D electron gas. A way to interpret with a topological point of view this quantization was proposed in Ref. [247]: an integer-valued topological invariant, the Chern number, is associated to each band of the electron spectrum trough an integral of the so-called Berry curvature. The conductance of the system for a Fermi energy inside a band gap is directly linked to these topological invariants.

The quantization of conductance for the integer quantum Hall effect is a single-particle effect. When taking into account interactions between electrons, one enters the fractional quantum Hall regime. It is characterized by plateaus of conductance with rational values of the quantum of conductance. In this regime, strongly correlated phases of matter appear due to the interplay between the non-trivial band structure and interactions between electrons. Several emblematic states are encountered in this regime like Laughlin [248] or Moore-Read states [249], which feature large scale entanglement or "exotic" fractional statistics for the quasi-particle like excitation.

Our motivation in the ytterbium project is to create analogous phases of matter with neutral atoms. More precisely, quantum Hall physics is often modelled by the Harper-Hofstadter hamiltonian which describes particles hoping on a tight-binding 2D lattice and subject to a transverse magnetic field. We aim at implementing this hamiltonian with neutral atoms. We will benefit from the versatility of ultracold atomic systems to provide new insights on this many-body physics problem. Creating a 2D system of particles moving in a lattice is routinely achieved in our community but the major challenge is to mimic the effect of orbital magnetism on neutral atoms, which are, because of their neutrality, naturally insensitive to such effects.

Several routes have been identified to create artificial magnetism. One of them is to set the system in rotation with a rotation vector $\mathbf{\Omega}$ and to exploit, for a particle of mass m, charge q and moving a velocity $\mathbf{v}$ the equivalence between Coriolis force ($m\mathbf{\Omega} \times \mathbf{v}$) and Lorentz force for a magnetic field $\mathbf{B}$ ($q\mathbf{v} \times \mathbf{B}$). Whereas this approach has been quite successful, entering the large magnetic field regime remains challenging because it corresponds to create a sample with a number of vortices comparable to the number of atoms [250, 251, 30]. A second route to induce artificial magnetism is to engineer atomic states dressed by a laser potential. For a proper laser geometry, atoms moving in this potential will acquire a geometrical "Berry" phase that can be associated to an effective magnetic field [252, 253, 31]. An example of such a protocol has been reported in Ref. [254] and characterized by the detection of vortices in the cloud. However, this protocol is plagued by a spontaneous emission rate large compared to the relevant energy sales in this kind of experiments and rather unavoidable with alkalis. It thus limits the perspectives to study strongly correlated phases of matter with this protocol.

Protocols based on rotation and light-induced geometrical phases apply well to bulk systems. Here, we are interested mostly in lattice systems and our research plans are based on a protocol originating from Ref. [33] which has been adapted to ytterbium atoms in superlattices potentials [34]. Briefly, this protocol is based on the control of the phase of tunnel matrix elements by the optical clock laser described in the previous chapter. The control of this phase leads to the possibility to engineer the value of the effective

magnetic flux piercing a given lattice plaquette.

3.4.2 State of the art

Realization of topological bands in artificial materials has been the focus of an extremely intense activity in the last few years. These efforts include important development in photonics, atomic physics or other metamaterials and a detailed description can be found in recent reviews [255, 256, 32]. Here, we focus on a brief review of recent achievements in lattice systems with ultracold atoms. We first focus on experiments probing single-particle physics. Their motivation is thus to probe the topology of the band structure and they do not deal with the realization of many-body phases. Second, we describe recent achievements in the understanding of the role of interactions and the realization of topological many-body phases.

1D systems An emblematic model of a topological lattice is the SSH model [32], inspired from the modelling of the polyacetylene molecule [257]. This model describes a 1D lattice system in the tight-binding approximation where the tunnelling elements alternate in space between two values. This model was realized in Ref. [258] by creating a 1D superlattice. This superlattice results from the controlled superposition of a standard optical lattice with a second one at a doubled wavelength so that one gets a lattice of double wells. The relative amplitude of the tunnelling elements (inside the double well- or between neighbouring double wells) is tuned thanks to the relative spatial phase of the two lattices. With this settings, the topology of the system was revealed by a measurement of the Zak phase [258]. This Zak phase is not a "robust" topological invariant[1] and it is not connected to transport properties, contrary to the Chern number which is related to th transverse conductance in 2D Hall systems. There is thus a strong motivation for investigating two-dimensional systems.

"Extended" 1D systems An interesting approach to realize two dimensional topological systems is to use a 1D system in space and to use the internal states space as a second effective dimension [259]. Tunnelling in this effective dimension is controlled by Raman coupling between the different internal states. This effective dimension is thus limited to a small value (typically 3 to 5 in current experiments) but many features of the underlying topology could be probed. First experiments have been described in [260, 261] and a recent experiment has reported the observation of topological edge states in this system [262]. Importantly, the role of interactions in this kind of protocol differs from the usual short-range interactions. Indeed, along the synthetic dimension, interactions are driven by the Raman transitions and are thus of infinite range [263, 264].

Another situation where topological properties can be described is also in systems with one dimension of space and where time is playing the role of the second dimension. This situation is encountered in topological pumps, first proposed by Thouless [265]. Topological pumping appears as a net quantized motion of the particle during a cyclic adiabatic evolution (pumping) of the system. Such pumps have been demonstrated for bosons and fermions in Refs. [266, 267].

2D systems Artificial magnetism has also been demonstrated at the single-particle level in "true" 2D systems. In these experiments a lattice of 1D tubes is created and several techniques are used to induce complex tunnelling elements between the different sites of the lattice. The realization of Harper-Hofstadter or Haldane [268] hamiltonians have been obtained with such procedures.

[1] only relative phases are meaningful.

The general idea is to start from a lattice configuration with almost no tunnelling and then to restore tunnelling thanks to a proper time modulation of the lattice. All the experiments reported so far were realized with a single internal state. Complex tunnelling elements have been obtained mainly with two different methods. A first possibility is to use an additional running wave laser. As the phase of the laser varies on the scale of the lattice period it is possible to control the phase of the (complex) effective tunnelling amplitude. This idea has been used to create staggered flux [269] and uniform flux in a square lattice [270, 271, 272]. Another possibility is to time modulate the lattice to create effective complex tunnelling elements [273, 274]. This protocol has been used to create artificial gauge fields [275] and realize a staggered flux [276]. It has also been used to implement the Haldane model in an honeycomb lattice [277]. Bands with a non-zero local Berry curvature have also been realized by a circular shaking of an hexagonal lattice [278].

Other recent experiments on artificial gauge fields with quantum gases Integer quantum Hall effect appears for even values of the dimension of space. Using artificial systems, quantum Hall physics can be extended to four dimensions as recently demonstrated in Ref. [279]. A 2D system is subjected to topological pumping in both direction of space thus leading to dynamical 4D physics with two dimensions of space and two dimensions of "phase" of the pumps.

Non-trivial phases of matter can also be obtained when applying spin-orbit coupling. Experiments with 1D spin-orbit coupling [280, 281, 282] have been recently extended to 2D [283, 284] and topology of the band structure has been characterized [285]. These protocols do not apply to the tight-binding regime and are closely related to the concept of flux lattices which was introduced in [286, 287] to create topological bands using light dressed states with weak optical lattice.

Interactions A large heating is usually observed in the experiments studying bosons in 2D topological bands. For instance, in Ref. [272] with a uniform magnetic field, several bands are populated when applying the synthetic magnetic field. This heating originates from the time modulation whose frequency is not large enough compare to the typical energies of the system. Indeed, one is limited to a modulation lower than the energy gap to avoid interband transitions and operate the system in the ground band. For these typical modulation frequencies, several studies pointed out the role of interactions between particles [288, 289, 290]. Such interactions are able to transfer energy from the (fast) micromotion induced by the time modulation to slowly-varying degrees of freedom, hence leading to heating.

Despite this strong heating a Bose-Einstein condensate has been loaded in the ground-band of the lattice [269, 275, 291]. However in all these cases the magnetic flux is staggered meaning that there are no global topological properties in these systems.

3.4.3 Description of our protocol to induce artificial magnetism

The basic idea

In quantum mechanics, a particle of charge q moving in magnetic field $\mathbf{B}$ on a closed loop acquires a Aharonov-Bohm phase

$$\Phi_{\mathrm{AB}} = \frac{q}{\hbar} \iint \mathbf{B}.\mathbf{dS}, \tag{3.1}$$

where the integral is the flux of the magnetic field through the loop defined by the trajectory of the particle. Artificial orbital magnetism for a neutral particle can be obtained by controlling the phase

evolution of this particle on a closed loop. In the protocol described below we use optical coherent coupling between two internal states of ytterbium atoms to imprint such a phase.

Description of the protocol

Consider a two-state atom, confined in a 2D plane and trapped in a bichromatic optical square lattice (see Fig. 3.5). Along the y direction the lattice is created by the interference of a laser beam which creates the same potential for both internal states (thus operating at the magic wavelength λ_m). Lattice sites are separated by the distance $d_y = \lambda_\mathrm{m}/2$. Along the x direction the lattice creates an opposite potential for both internal states (thus operating at an "anti-magic" wavelength λ_am). The distance between two sites for the two different internal states is thus $d_x = \lambda_\mathrm{am}/4$. In the protocol, tunnelling along the y-direction is controlled by the lattice depth and the corresponding matrix element is real. The depth of the anti-magic wavelength is chosen to be large enough to suppress tunnelling along the x-direction (for both internal states).

The key ingredient to create artificial magnetism is to add laser-induced tunnelling. A laser, tuned to the transition between the two internal states, induces hopping. The effective matrix tunnel element depends on the phase $\mathbf{k}_\mathrm{c}.\mathbf{r}$ of the laser of wavevector $\mathbf{k}_\mathrm{c}$ ($k_c = 2\pi/\lambda_c$) and can thus be complex. The system can then be described by the tight-binding Hofstadter-Harper hamiltonian [34]

$$H_\mathrm{HH} = -J \sum_{n,m,\pm} e^{2i\pi\alpha m} \hat{c}^\dagger_{n\pm1,m} \hat{c}_{n,m} + \hat{c}^\dagger_{n,m\pm1} \hat{c}_{n,m} + \mathrm{h.c.}, \tag{3.2}$$

where J is the tunnel energy. The operator $\hat{c}^\dagger_{n,m}$ creates a particle at position $(x, y) = (nd_x, md_y)$ where n and m are the lattice site indices. The phase associated to hopping along the x direction depends on the dimensionless effective magnetic field flux $\alpha = d_y/\lambda_\mathrm{c}$ (expressed in units of 2π). This can be seen more clearly when considering the motion of a particle along the edges of a single plaquette of the lattice. The phase accumulated by the particle after a loop is, for $\mathbf{k}_\mathrm{c} \parallel \mathbf{x}$, $\Phi = 2\pi\lambda_\mathrm{m}/(2\lambda_\mathrm{c})$ (see Fig. 3.5). For our experimental parameters this phase is larger than π and can be tuned to any lower value by changing the angle of the clock laser with respect to the lattice axes.

With this configuration one can see that the flux is not the same for all the plaquettes and its value alternates along x from positive to opposite negative values. Whereas such a staggered flux could be interesting, we aim at realizing a uniform flux. We will add along the x axis an additional laser at twice the antimagic wavelength. This potential has a period doubled compared to the antimagic lattice and will thus lift the degeneracy of the coherent coupling resonance frequencies between the odd plaquettes with a positive flux and the even plaquettes with a negative flux. To obtain an opposite flux for, *e.g.*, the even plaquettes one should use a clock laser propagating along $-\mathbf{x}$ and with the correct frequencies (shifted by the superlattice potential). More details can be found in Ref. [34].

Implementation with ytterbium atoms

Ytterbium atom is well-adapted for this protocol because of the existence of the clock transition at $\lambda_\mathrm{c} = 578\,\mathrm{nm}$. In addition, the atom should offer suitable magic and anti-magic wavelengths. We use in our team $\lambda_\mathrm{m} = 760\,\mathrm{nm}$ and $\lambda_\mathrm{am} = 612\,\mathrm{nm}$ (and thus $2\lambda_\mathrm{am} = 1224\,\mathrm{nm}$). One limitation of ytterbium is the large value of the inelastic loss rate between atoms in the metastable state that we have measured in Ref. [239]. We should thus limit ourselves to situation with a low density in the metastable state. Note that, the inelastic loss rate between ground and metastable state is low enough to be irrelevant in our range of parameters.

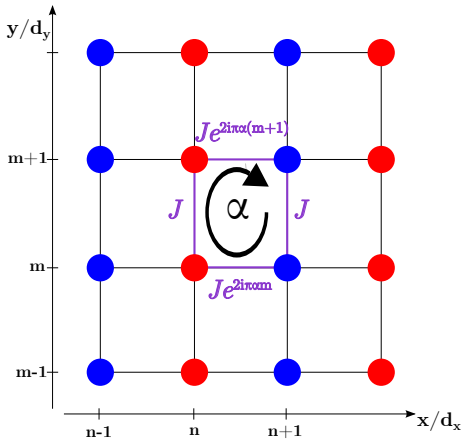

Figure 3.5: *Protocol for implementing an artificial magnetic field. Two internal states of the ytterbium atom, depicted as blue and red disks, are trapped in alternating columns of a 2D lattice. Tunnelling along the y direction happens with a real coupling constant J. Tunnelling along the x direction is induced by a laser which imprints its spatial phase on the corresponding tunnelling element which becomes complex and spatially dependent. When a particle hops around the central plaquette, it acquires a effective phase $2\pi\alpha$ which simulates an artificial magnetic field.*

As described in the previous chapter we currently have most of the tools to implement the above described protocol. In the near future we plan to implement the following upgrades:

- One of arm of the in-plane lattice, currently operating at the magic wavelength, should be switched to the anti-magic wavelength. For this purpose we have developed a frequency-doubling system outputting laser light at 612 nm and which is ready to be used. The necessary superlattice can be realized with this system by combining frequency-doubled light with the fundamental light. Thanks to frequency doubling the two laser lights are automatically phase locked.
- Even if our protocol can be implemented in a stack of 2D clouds as described in the previous chapter, or in a 2D lattice of 1D tubes (by just removing the vertical lattice), we wish to operate with a single 2D lattice. This will allow us to probe accurately the main properties of quantum Hall states, like incompressibility, that are usually washed out when integrating over several clouds. We have thus planned the installation of an additional dipole trap to create a single 2D cloud (similarly to what has been described in chapter 1) that will subsequently be loaded around a single node of the vertical magic lattice.
- Finally, we have developed an home-made microscope objective to enable optical imaging with a sub-micron resolution. This will facilitate the characterization of the realized phases and will also allow us to realize potential engineering of the external trapping potential to favour the apparition of low-entropy phases like described in Refs. [35, 19].

3.4.4 Expected results

The implementation of this protocol will be accompanied with the characterization of the realized hamiltonian. We will first focus on single particle physics and the characterization of the topological properties underlying this hamiltonian. Then, we will explore the many-body equilibrium state of an assembly of cold atoms (first bosons but also fermions at a longer term) in this topological band structure.

Single-particle physics: Probing the topology of the bands

The band structure of the Harper-Hofstadter hamiltonian for different values of the magnetic flux is known as the Hofstadter butterfly [292] and presents a wealth of mathematical properties like a fractal structure. By tuning the angle of the clock laser with respect to the lattice we will be able to probe this band structure which could be revealed, using bosons, by a measuring the momentum distribution in time-of-flight experiments [34].

More challenging is to probe the topology of the bands. Topology could be determined from the Berry curvature of the bands. Its integral over the Brillouin gives directly the Chern number associated to this band. A protocol to measure the Berry curvature was proposed in Ref. [293] based on the "anomalous" drift of an atomic wavepacket driven by an external force, in strong analogy to the transverse current observed in a classical Hall effect experiment. This approach has already been used in several experiments, for instance to determine Chern numbers in Ref. [272] or to characterize Dirac cones in graphene-like band structures [294, 295].

Another possibility is to observe the so-called "edge states" at the boundary of the system. It has been shown, for a finite-size system, that the topology of the band structure is reflected by the presence of edge states in the energy band gap. These states are localized at the boundary of the system and have a given chirality, *i.e.*, the associated group velocity of the state has a fixed direction along the edge of the system. The so-called "bulk-edge" correspondence ensures the presence of such states for a topological band structure. In the context of quantum Hall effect, the measured conductance when the Fermi energy is tuned inside an energy gap is due to conduction of electrons in these modes (and not in the bulk of the material). Several methods to observe these modes in quantum gases experiments have been proposed [296]. In our team, in collaboration with N. Goldman we have proposed to observe such states using Bragg spectroscopy with the clock laser [297, 298]. This protocol allows one to directly image *in situ* these edge states and to probe their chirality and dispersion relation.

Many other methods have been proposed to characterize topological band structures, for instance based on measurements after time-of-flight. We cannot review all of them in this document and refer to a recent review [299].

Many-body physics

What is the equilibrium state of gas of interacting bosons on an optical lattice and subject to an artificial magnetic field? Answering this question in its full generality is a theoretical challenge and the realization of precise experiments on this subject is crucial to push our knowledge forward. Several parameters influence the phase diagram of this system. First, there is obviously the magnetic flux α. Because of the fractal structure of the Hofstadter spectrum the equilibrium state strongly depends on it. The other parameters are the typical energy scales of the Bose-Hubbard model: Tunnelling energy J, on-site interaction U, and chemical potential μ. Finally, the role of finite temperature/entropy that is not well controlled in experiments is likely to be important. Temperature could be comparable to the energy gap of the many-body phases. We do not want to review the details of this phase diagram and we focus on two (experimentally relevant) situations.

For a weak lattice, so that the on-site interaction energy remains small compared to the kinetic energy ($U \ll J$), a superfluid phase is expected, similarly to the case of the Bose-Hubbard model. However, the presence of the artificial magnetic field leads to the generation of vortices. For low enough temperature, the vortices should arrange in a vortex lattice, as the Abrikosov lattice in the absence of magnetic field [8, 300]. However, this vortex lattice will be influenced by the presence of the optical lattice which frustrates the vortex lattice [301].

The main motivation is to realize fractional quantum Hall states with this system. These states appears for strong interactions and for specific filling factors (1/2 for a Laughlin state of bosons) [2]. A specific "hole Laughlin state" has also been predicted near (for instance) the $n = 1$ Mott plateau in [302]: it consists in a set of holes moving in a bath of atoms forming a $n = 1$ Mott phase. These fractional quantum Hall states are incompressible and may be revealed as "mini" plateaus in the wedding-cake structure of the density profile of a trapped Mott insulator, as usually observed in optical lattice experiments [303]. However the width of these plateaus is expected to be small and thus difficult to observe without a good control of the trap profile. In our experiment, we plan to engineer the trap profile using a spatial light modulator, similarly to what is been done recently to observe antiferromagnetic states in low-entropy optical lattices [35, 19]

3.5 Topological properties of 1D quasicrystals.

This study is published in Ref. [304].

In parallel to our work on ytterbium quantum gases, we have realized an optical diffraction experiment on quasi-periodic gratings. These gratings have been realized thanks to the use of spatial light modulators as described in Chapter 1, which allow us to tune easily the grating. We have shown that topological invariants that characterizes quasi-periodic chains and the fractal structure of their spectra can be measured with a simple optical setup. There is a strong link between topological properties of 1D quasi-periodic systems and those of the Harper model [305]. This work, that we will not detail more here, has been realized in collaboration with E. Akkermans and E. Levy from Technion in Israël.

3.6 Conclusion

We have constructed a new experimental system to manipulate ytterbium quantum gases in optical lattices. In parallel, we have developed an ultranarrow laser system similar to the one used in optical clocks. With this system we have realized a set of original experiments of spectroscopy of quantum gases with a clock laser. This allowed us to investigate many-body dynamics in a driven two-mode BEC and to determine the previously unknown collisional parameters of ^{174}Yb. I have also described how we plan to create artificial magnetism on this setup taking advantage of the presence of the optical clock transition. Our experimental apparatus is now quite well-developed and we have all the building blocks ready to tackle the realization of the proposal of Ref. [34]. We aim at preparing topological many-body phases, like bosonic quantum Hall states. This goes beyond the state of the art which is so far mostly limited to the observation of single-particle effects because of the large heating observed in the experiments.

[2] The filling factor is given by the ratio of the on-site atom number and the magnetic flux.

Conclusion

During the ten years I have spent at Laboratoire Kastler Brossel, I have contributed to the development of two new experimental setups that are now operated at Collège de France after a move from Ecole Normale Supérieure. These two apparatus are dedicated to the investigation of quantum many-body physics with ultracold quantum gases. We have seen that topological phenomena plays a central role in this work and the future research plans.

One project focuses on the 2D Bose gas. We have built an apparatus which allows us to confine rubidium atoms into a single layer with an arbitrary in-plane potential. We have demonstrated the realization of uniform 2D Bose gases and study their coherence, the formation of vortices after quench cooling and their superfluid behavior via the measurement of speed of sound. We have also tailored the geometry to study the stochastic formation of supercurrents in a ring configuration, after quench cooling and after the merging of independent BECs. This setup also allowed us to investigate light scattering in a dense regime where many atoms are confined on the scale given by the light wavelength and thus interact collectively. In the future, we plan to keep on investigating physics in 2D systems, for instance to observe the algebraic decay of the first-order correlation function and if possible to study the dynamical crossing of the BKT phase transition. We also plan to upgrade our apparatus to start studying mixtures of different hyperfine states. We will explore superfluid hydrodynamics in a mixture and we will investigate impurity dynamics with the objective of implementing the quantum Brownian motion model.

The other project is dedicated to the physics of atoms in optical lattices. We have developed an ytterbium BEC machine to benefit specifically from the existence of a clock transition in the atomic spectrum of the ytterbium atom. We have built a clock laser to drive this ultranarrow transition and we have demonstrated the spectroscopy of quantum gases of ytterbium atoms with this clock laser. We have probed an ytterbium BEC trapped in a optical dipole trap operating at the magic wavelength and study its rich dynamics under coherent driving. We also determined all the relevant elastic and inelastic scattering cross sections of ytterbium atoms in the ground and metastable state thanks to the spectroscopy of single atoms or pairs of atoms confined in a 3D optical lattice. In the near future we will address the realization of artificial gauge fields with this setup, which is the original motivation for the building of the apparatus. Using the clock laser we will control the phase of the hopping elements in a 2D optical lattice in a way that will mimic the orbital effect of a magnetic field on charged particles. This will allow us to study many-body phases in topological bands thus opening the possibility to realize strongly correlated phases, which will be the bosonic equivalents of fractional quantum Hall phases observed in electron gases.

In summary, we have developed powerful experimental platforms which have already demonstrated their originality. We will use these tools to deepen our exploration of quantum many-body phases of matter. The most challenging and intriguing research lines will focus on dynamical phenomena and strongly correlated phases of matter. In all situations we expect that the underlying topology will play an important role.

Bibliography

[1] N. Saquet, A. Cournol, J. Beugnon, J. Robert, P. Pillet, and N. Vanhaecke. Landau-Zener transitions in frozen pairs of Rydberg atoms. *Phys. Rev. Lett.*, 104:133003, 2010.

[2] Y. Tokura, M. Kawasaki, and N. Nagaosa. Emergent functions of quantum materials. *Nat. Phys.*, 13(11):1056, 2017.

[3] B Keimer and JE Moore. The physics of quantum materials. *Nat. Phys.*, 13(11):1045, 2017.

[4] K.R. Atkins. *Liquid Helium*. Cambdrige University Press, 2014.

[5] M.H. Anderson, J.R. Ensher, M.R. Matthews, C.E. Wieman, and E.A. Cornell. Observation of Bose-Einstein condensation in a dilute atomic vapor. *Science*, 269(5221):198–201, 1995.

[6] K. B. Davis, M.-O. Mewes, M.R. Andrews, N.J. van Druten, D.S. Durfee, D.M. Kurn, and W. Ketterle. Bose-Einstein condensation in a gas of Sodium atoms. *Phys. Rev. Lett.*, 75:3969–3973, 1995.

[7] R. Onofrio, C. Raman, J. Vogels, J. Abo-Shaeer, A. Chikkatur, and W. Ketterle. Observation of superfluid flow in a bose-einstein condensed gas. *Phys. Rev. Lett.*, 85:2228–2231, 2000.

[8] K.W. Madison, F. Chevy, W. Wohlleben, and J. Dalibard. Vortex formation in a stirred Bose-Einstein condensate. *Phys. Rev. Lett.*, 84(5):806, 2000.

[9] S. Inouye, S. Gupta, T. Rosenband, A. Chikkatur, A. Görlitz, T. Gustavson, A. Leanhardt, D. Pritchard, and W. Ketterle. Observation of vortex phase singularities in bose-einstein condensates. *Phys. Rev. Lett.*, 87:080402, 2001.

[10] D. Stamper-Kurn, A. Chikkatur, A. Görlitz, S. Inouye, S. Gupta, D. Pritchard, and W. Ketterle. Excitation of phonons in a Bose-Einstein condensate by light scattering. *Phys. Rev. Lett.*, 83:2876–2879, 1999.

[11] C.A. Regal, C. Ticknor, J.L. Bohn, and D.S. Jin. Creation of ultracold molecules from a Fermi gas of atoms. *Nature*, 424(6944):47–50, 2003.

[12] A. Görlitz, J. Vogels, A. Leanhardt, C. Raman, T. Gustavson, J. Abo-Shaeer, A. Chikkatur, S. Gupta, S. Inouye, T. Rosenband, and W. Ketterle. Realization of Bose-Einstein condensates in lower dimensions. *Phys. Rev. Lett.*, 87:130402, 2001.

[13] K. Henderson, C. Ryu, C. MacCormick, and M.G. Boshier. Experimental demonstration of painting arbitrary and dynamic potentials for Bose–Einstein condensates. *New J. Phys.*, 11(4):043030, 2009.

[14] M. Mestre, F. Diry, B. Viaris de Lesegno, and L. Pruvost. Cold atom guidance by a holographically-generated Laguerre-Gaussian laser mode. *Eur. Phys. J. D*, 57(1):87–94, 2010.

[15] L. Corman, L. Chomaz, T. Bienaimé, R. Desbuquois, C. Weitenberg, S. Nascimbène, J. Dalibard, and J. Beugnon. Quench-induced supercurrents in an annular Bose gas. *Phys. Rev. Lett.*, 113:135302, 2014.

[16] L. Chomaz, L. Corman, T. Bienaimé, R. Desbuquois, C. Weitenberg, S. Nascimbène, J. Beugnon, and J. Dalibard. Emergence of coherence via transverse condensation in a uniform quasi-two-dimensional Bose gas. *Nat. Comm.*, 6(6):6162, 2015.

[17] N. Navon, A.L. Gaunt, R.P. Smith, and Z. Hadzibabic. Critical dynamics of spontaneous symmetry breaking in a homogeneous Bose gas. *Science*, 347(6218):167–170, 2015.

[18] G. Gauthier, I. Lenton, N.M. Parry, M. Baker, M.J. Davis, H. Rubinsztein-Dunlop, and T.W. Neely. Direct imaging of a digital-micromirror device for configurable microscopic optical potentials. *Optica*, 3(10):1136–1143, 2016.

[19] C. S. Chiu, G. Ji, A. Mazurenko, D. Greif, and M. Greiner. Quantum state engineering of a Hubbard system with ultracold fermions. *Phys. Rev. Lett.*, 120:243201, 2018.

[20] I. Bloch. Ultracold quantum gases in optical lattices. *Nat. Phys.*, 1:23–30, 2005.

[21] P. Courteille, R.S. Freeland, D.J. Heinzen, F.A. van Abeelen, and B.J. Verhaar. Observation of a Feshbach resonance in cold atom scattering. *Phys. Rev. Lett.*, 81:69–72, 1998.

[22] M. Schreiber, S.S. Hodgman, P. Bordia, H.P. Lüschen, M.H. Fischer, R. Vosk, E. Altman, U. Schneider, and I. Bloch. Observation of many-body localization of interacting fermions in a quasi-random optical lattice. *Science*, page 7432, 2015.

[23] A.Y. Kitaev. Unpaired Majorana fermions in quantum wires. *Physics-Uspekhi*, 44(10S):131, 2001.

[24] P. St-Jean, V. Goblot, E. Galopin, A. Lemaître, T. Ozawa, L. Le Gratiet, I. Sagnes, J. Bloch, and A. Amo. Lasing in topological edge states of a one-dimensional lattice. *Nat. Photonics*, 11(10):651, 2017.

[25] G. Harari, M.A. Bandres, Y. Lumer, M.C. Rechtsman, Y.D. Chong, M. Khajavikhan, D.N. Christodoulides, and M. Segev. Topological insulator laser: Theory. *Science*, 359(6381):4003, 2018.

[26] M.A. Bandres, S. Wittek, G. Harari, M. Parto, J. Ren, M. Segev, D.N. Christodoulides, and M. Khajavikhan. Topological insulator laser: Experiments. *Science*, 359(6381):4005, 2018.

[27] J.M. Kosterlitz. Nobel lecture: Topological defects and phase transitions. *Rev. Mod. Phys.*, 89:040501, 2017.

[28] M. Ueda. Topological aspects in spinor Bose–Einstein condensates. *Rep. Prog. Phys.*, 77(12):122401, 2014.

[29] T. Ando, A. Fowler, and F. Stern. Electronic properties of two-dimensional systems. *Rev. Mod. Phys.*, 54:437–672, 1982.

[30] N.R. Cooper. Rapidly rotating atomic gases. *Adv. Phys.*, 57(6):539–616, 2008.

[31] J. Dalibard, F. Gerbier, G. Juzeliūnas, and P. Öhberg. *Colloquium*: Artificial gauge potentials for neutral atoms. *Rev. Mod. Phys.*, 83:1523–1543, 2011.

[32] N.R. Cooper, J. Dalibard, and I.B. Spielman. Topological bands for ultracold atoms. *arXiv:1803.00249*, 2018.

[33] D. Jaksch and P. Zoller. Creation of effective magnetic fields in optical lattices: the Hofstadter butterfly for cold neutral atoms. *New J. Phys.*, 5(1):56, 2003.

[34] F. Gerbier and J. Dalibard. Gauge fields for ultracold atoms in optical superlattices. *New J. Phys.*, 12(3):033007, 2010.

[35] A. Mazurenko, C.S. Chiu, G. Ji, M.F. Parsons, M. Kanász-Nagy, R. Schmidt, F. Grusdt, E. Demler, D. Greif, and M. Greiner. A cold-atom Fermi–Hubbard antiferromagnet. *Nature*, 545(7655):462, 2017.

[36] J. Billy, V. Josse, Z. Zuo, A. Bernard, B.; Hambrecht, P. Lugan, D. Clément, L. Sanchez-Palencia, P. Bouyer, and A. Aspect. Direct observation of Anderson localization of matter waves in a controlled disorder. *Nature*, 453(7197):891, 2008.

[37] G. Roati, C. D'Errico, L. Fallani, M. Fattori, C. Fort, M. Zaccanti, G. Modugno, M. Modugno, and M. Inguscio. Anderson localization of a non-interacting Bose–Einstein condensate. *Nature*, 453(7197):895, 2008.

[38] G. Quéméner and P.S. Julienne. Ultracold molecules under control! *Chem. Rev.*, 112(9):4949–5011, 2012.

[39] A.D. Ludlow, M.M. Boyd, J. Ye, E. Peik, and P.O. Schmidt. Optical atomic clocks. *Rev. Mod. Phys.*, 87(2):637, 2015.

[40] Z. Hadzibabic, P. Krüger, M. Cheneau, B. Battelier, and J. Dalibard. Berezinskii–Kosterlitz–Thouless crossover in a trapped atomic gas. *Nature*, 441(7097):1118, 2006.

[41] V. Schweikhard, S. Tung, and E.A. Cornell. Vortex proliferation in the Berezinskii-Kosterlitz-Thouless regime on a two-dimensional lattice of Bose-Einstein condensates. *Phys. Rev. Lett.*, 99:030401, 2007.

[42] P. Cladé, C. Ryu, A. Ramanathan, K. Helmerson, and W.D. Phillips. Observation of a 2D Bose gas: From thermal to quasicondensate to superfluid. *Phys. Rev. Lett.*, 102:170401, 2009.

[43] S. Tung, G. Lamporesi, D. Lobser, L. Xia, and E.A. Cornell. Observation of the presuperfluid regime in a two-dimensional Bose gas. *Phys. Rev. Lett.*, 105:230408, 2010.

[44] P.A. Murthy, I. Boettcher, L. Bayha, M. Holzmann, D. Kedar, M. Neidig, M.G. Ries, A.N. Wenz, G. Zürn, and S. Jochim. Observation of the Berezinskii-Kosterlitz-Thouless phase transition in an ultracold Fermi gas. *Phys. Rev. Lett.*, 115:010401, 2015.

[45] Z. Hadzibabic and J. Dalibard. Two-dimensional Bose fluids: An atomic physics perspective. *Rivista del Nuovo Cimento*, 34:389, 2011.

[46] D.J. Bishop and J.D. Reppy. Study of the superfluid transition in two-dimensional ^{4}He films. *Phys. Rev. Lett.*, 40:1727–1730, 1978.

[47] P.C. Hohenberg. Existence of long-range order in one and two dimensions. *Phys. Rev.*, 158:383–386, 1967.

[48] N.D. Mermin and H. Wagner. Absence of ferromagnetism or antiferromagnetism in one- or two-dimensional isotropic Heisenberg models. *Phys. Rev. Lett.*, 17:1307–1307, 1966.

[49] J.-y. Choi, S.W. Seo, and Y.-i. Shin. Observation of thermally activated vortex pairs in a quasi-2d Bose gas. *Phys. Rev. Lett.*, 110(17):175302, 2013.

[50] M.E. Cage, K. von Klitzing, A.M. Chang, F. Duncan, M. Haldane, R.B. Laughlin, A.M.M. Pruisken, and D.J. Thouless. *The quantum Hall effect*. Springer Science & Business Media, 2012.

[51] Desbuquois R. *Thermal and superfluid properties of the two-dimensional Bose gas*. PhD thesis, Université Pierre et Marie Curie, 2013.

[52] Chomaz L. *Coherence and superfluidity of Bose gases in reduced dimensions: from harmonic traps to uniform fluids*. PhD thesis, Ecole Normale Supérieure, 2014.

[53] Corman L. *The two-dimensional Bose gas in box potentials*. PhD thesis, PSL Research University, 2016.

[54] Ville J.L. *Quantum gases in box potentials: Sound and light in bosonic Flatland*. PhD thesis, PSL Research University, 2018.

[55] J. Dalibard. Cours du Collège de France, Fluides quantiques de basse dimension et transition de Kosterlitz-Thouless. 2017.

[56] L.-C. Ha, C.-L. Hung, X. Zhang, U. Eismann, S.-K. Tung, and C. Chin. Strongly interacting two-dimensional Bose gases. *Phys. Rev. Lett.*, 110:145302, 2013.

[57] B. Fröhlich, M. Feld, E. Vogt, M. Koschorreck, W. Zwerger, and M. Köhl. Radio-frequency spectroscopy of a strongly interacting two-dimensional Fermi gas. *Phys. Rev. Lett.*, 106:105301, 2011.

[58] P.A. Murthy, D. Kedar, T. Lompe, M. Neidig, M.G. Ries, A.N. Wenz, G. Zürn, and S. Jochim. Matter-wave Fourier optics with a strongly interacting two-dimensional Fermi gas. *Phys. Rev. A*, 90:043611, 2014.

[59] C. Mora and Y. Castin. Extension of Bogoliubov theory to quasicondensates. *Phys. Rev. A*, 67:053615, 2003.

[60] N. Prokof'ev and B. Svistunov. Two-dimensional weakly interacting Bose gas in the fluctuation region. *Phys. Rev. A*, 66:043608, 2002.

[61] G.E. Astrakharchik, J. Boronat, J. Casulleras, I.L. Kurbakov, and Yu.E. Lozovik. Equation of state of a weakly interacting two-dimensional Bose gas studied at zero temperature by means of quantum Monte Carlo methods. *Phys. Rev. A*, 79:051602, 2009.

[62] T. Yefsah, R. Desbuquois, L. Chomaz, K.J. Günter, and J. Dalibard. Exploring the thermodynamics of a two-dimensional Bose gas. *Phys. Rev. Lett.*, 107:130401, 2011.

[63] C.-L. Hung, X. Zhang, N. Gemelke, and C. Chin. Observation of scale invariance and universality in two-dimensional Bose gases. *Nature*, 470(7333):236–239, 2011.

[64] R. Desbuquois, T. Yefsah, L. Chomaz, C. Weitenberg, L. Corman, S. Nascimbène, and J. Dalibard. Determination of scale-invariant equations of state without fitting parameters: Application to the two-dimensional Bose gas across the Berezinskii-Kosterlitz-Thouless transition. *Phys. Rev. Lett.*, 113:020404, 2014.

[65] I. Boettcher, L. Bayha, D. Kedar, P.A. Murthy, M. Neidig, M.G. Ries, A.N. Wenz, G. Zürn, S. Jochim, and T. Enss. Equation of state of ultracold fermions in the 2D BEC-BCS crossover region. *Phys. Rev. Lett.*, 116:045303, 2016.

[66] K. Fenech, P. Dyke, T. Peppler, M.G. Lingham, S. Hoinka, H. Hu, and C.J. Vale. Thermodynamics of an attractive 2D Fermi gas. *Phys. Rev. Lett.*, 116:045302, 2016.

[67] S.P. Rath, T. Yefsah, K.J. Günter, M. Cheneau, R. Desbuquois, M. Holzmann, W. Krauth, and J. Dalibard. Equilibrium state of a trapped two-dimensional Bose gas. *Phys. Rev. A*, 82:013609, 2010.

[68] S. Stock, Z. Hadzibabic, B. Battelier, M. Cheneau, and J. Dalibard. Observation of phase defects in quasi-two-dimensional Bose-Einstein condensates. *Phys. Rev. Lett.*, 95:190403, 2005.

[69] J.L. Ville, T. Bienaimé, R. Saint-Jalm, L. Corman, M. Aidelsburger, L. Chomaz, K. Kleinlein, D. Perconte, S. Nascimbène, J. Dalibard, and J. Beugnon. Loading and compression of a single two-dimensional Bose gas in an optical accordion. *Phys. Rev. A*, 95:013632, 2017.

[70] K. Merloti, R. Dubessy, L. Longchambon, A. Perrin, P.-E. Pottie, V. Lorent, and H. Perrin. A two-dimensional quantum gas in a magnetic trap. *New J. Phys.*, 15(3):033007, 2013.

[71] S.P. Johnstone, A.J. Groszek, P.T. Starkey, C.J. Billington, T.P. Simula, and K. Helmerson. Negative absolute temperatures of vortices in a two-dimensional superfluid. *arXiv:1801.06952*, 2018.

[72] K. Hueck, N. Luick, L. Sobirey, J. Siegl, T. Lompe, and H. Moritz. Two-dimensional homogeneous Fermi gases. *Phys. Rev. Lett.*, 120:060402, 2018.

[73] R. Desbuquois, L. Chomaz, T. Yefsah, J Léonard, J. Beugnon, C. Weitenberg, and J. Dalibard. Superfluid behaviour of a two-dimensional Bose gas. *Nat. Phys.*, 8:645–648, 2012.

[74] C. Raman, M. Köhl, R. Onofrio, D.S. Durfee, C.E. Kuklewicz, Z. Hadzibabic, and W. Ketterle. Evidence for a critical velocity in a Bose-Einstein condensed gas. *Phys. Rev. Lett.*, 83:2502–2505, 1999.

[75] D.E. Miller, J.K. Chin, C.A. Stan, Y. Liu, W. Setiawan, C. Sanner, and W. Ketterle. Critical velocity for superfluid flow across the BEC-BCS crossover. *Phys. Rev. Lett.*, 99:070402, 2007.

[76] W. Weimer, K. Morgener, V.P. Singh, J. Siegl, K. Hueck, N. Luick, L. Mathey, and H. Moritz. Critical velocity in the BEC-BCS crossover. *Phys. Rev. Lett.*, 114:095301, 2015.

[77] M. Wenzel, F. Böttcher, J.-N. Schmidt, M. Eisenmann, T. Langen, T. Pfau, and I. Ferrier-Barbut. Anisotropic critical velocity of a dipolar superfluid. *arXiv:1804.04552*, 2018.

[78] V.P. Singh, C. Weitenberg, J. Dalibard, and L. Mathey. Superfluidity and relaxation dynamics of a laser-stirred two-dimensional Bose gas. *Phys. Rev. A*, 95:043631, 2017.

[79] C. De Rossi, R. Dubessy, K. Merloti, M. de Goër de Herve, T. Badr, A. Perrin, L. Longchambon, and H. Perrin. Probing superfluidity in a quasi two-dimensional Bose gas through its local dynamics. *New J. of Phys.*, 18(6):062001, 2016.

[80] N.J. van Druten and W. Ketterle. Two-step condensation of the ideal Bose gas in highly anisotropic traps. *Phys. Rev. Lett.*, 79:549–552, 1997.

[81] J. Armijo, T. Jacqmin, K. Kheruntsyan, and I. Bouchoule. Mapping out the quasicondensate transition through the dimensional crossover from one to three dimensions. *Phys. Rev. A*, 83:021605, 2011.

[82] W. RuGway, A.G. Manning, S.S. Hodgman, R.G. Dall, A.G. Truscott, T. Lamberton, and K.V. Kheruntsyan. Observation of transverse Bose-Einstein condensation via Hanbury Brown–Twiss correlations. *Phys. Rev. Lett.*, 111:093601, 2013.

[83] T.W.B. Kibble. Topology of cosmic domains and strings. *J. Phys. A. Math. Gen.*, 9(8):1387–1398, 1976.

[84] W.H. Zurek. Cosmological experiments in superfluid helium? *Nature*, 317:505, 1985.

[85] A. del Campo and W.H. Zurek. Universality of phase transition dynamics: Topological defects from symmetry breaking. *Int. J. Mod. Phys. A*, 29(8), 2014.

[86] G. Lamporesi, S. Donadello, S. Serafini, F. Dalfovo, and G. Ferrari. Spontaneous creation of Kibble-Zurek solitons in a Bose-Einstein condensate. *Nat. Phys.*, 9:656, 2013.

[87] A. del Campo, T.W.B. Kibble, and W.H. Zurek. Causality and non-equilibrium second-order phase transitions in inhomogeneous systems. *J. Phys. Condens. Matter*, 25(40):404210, 2013.

[88] J. Beugnon and N. Navon. Exploring the Kibble–Zurek mechanism with homogeneous Bose gases. *J. Phys. B*, 50(2):022002, 2017.

[89] J.L. Ville, R. Saint-Jalm, É. Le Cerf, M. Aidelsburger, S. Nascimbène, J. Dalibard, and J. Beugnon. Sound propagation in a uniform superfluid two-dimensional Bose gas. *arXiv:1804.04037*, 2018.

[90] R.J. Donnelly. The two-fluid theory and second sound in liquid helium. *Phys. Today*, 62(10):34–39, 2009.

[91] T. Ozawa and S. Stringari. Discontinuities in the first and second sound velocities at the Berezinskii-Kosterlitz-Thouless transition. *Phys. Rev. Lett.*, 112:025302, 2014.

[92] M. Ota and S. Stringari. Second sound in a two-dimensional Bose gas: From the weakly to the strongly interacting regime. *Phys. Rev. A*, 97:033604, 2018.

[93] M. Ota, F. Larcher, F. Dalfovo, L. Pitaevskii, N.P. Proukakis, and S. Stringari. Collisionless sound in a uniform two-dimensional Bose gas. *arXiv:1804.04032*, 2018.

[94] A. Cappellaro, F. Toigo, and L. Salasnich. Collisionless dynamics in two-dimensional bosonic gases. *arXiv:1807.02541*, 2018.

[95] L.P. Pitaevskii and S. Stringari. Landau damping in dilute Bose gases. *Phys. Lett. A*, 235(4):398–402, 1997.

[96] M.R. Andrews, D.M. Kurn, H.-J. Miesner, D.S. Durfee, C.G. Townsend, S. Inouye, and W. Ketterle. Propagation of sound in a Bose-Einstein condensate. *Phys. Rev. Lett.*, 79:553–556, 1997.

[97] R. Meppelink, S.B. Koller, and P. van der Straten. Sound propagation in a Bose-Einstein condensate at finite temperatures. *Phys. Rev. A*, 80:043605, 2009.

[98] J. Joseph, B. Clancy, L. Luo, J. Kinast, A. Turlapov, and J.E. Thomas. Measurement of sound velocity in a Fermi gas near a Feshbach resonance. *Phys. Rev. Lett.*, 98:170401, 2007.

[99] L.A. Sidorenkov, M.K. Tey, R. Grimm, Y.-H. Hou, L. Pitaevskii, and S. Stringari. Second sound and the superfluid fraction in a Fermi gas with resonant interactions. *Nature*, 498(7452):78–81, 2013.

[100] M. Aidelsburger, J. L. Ville, R. Saint-Jalm, S. Nascimbène, J. Dalibard, and J. Beugnon. Relaxation dynamics in the merging of *N* independent condensates. *Phys. Rev. Lett.*, 119:190403, 2017.

[101] A. Kumar, S. Eckel, F. Jendrzejewski, and G.K. Campbell. Temperature-induced decay of persistent currents in a superfluid ultracold gas. *Phys. Rev. A*, 95:021602, 2017.

[102] C. Ryu, M.F. Andersen, P. Cladé, V. Natarajan, K. Helmerson, and W.D. Phillips. Observation of persistent flow of a Bose-Einstein condensate in a toroidal trap. *Phys. Rev. Lett.*, 99:260401, 2007.

[103] A. Ramanathan, K.C. Wright, S.R. Muniz, M. Zelan, W.T. Hill, C.J. Lobb, K. Helmerson, W.D. Phillips, and G.K. Campbell. Superflow in a toroidal Bose-Einstein condensate: An atom circuit with a tunable weak link. *Phys. Rev. Lett.*, 106:130401, 2011.

[104] S. Moulder, S. Beattie, R.P. Smith, N. Tammuz, and Z. Hadzibabic. Quantized supercurrent decay in an annular Bose-Einstein condensate. *Phys. Rev. A*, 86:013629, 2012.

[105] K.C. Wright, R.B. Blakestad, C.J. Lobb, W.D. Phillips, and G.K. Campbell. Driving phase slips in a superfluid atom circuit with a rotating weak link. *Phys. Rev. Lett.*, 110:025302, 2013.

[106] K.C. Wright, R.B. Blakestad, C.J. Lobb, W.D. Phillips, and G.K. Campbell. Threshold for creating excitations in a stirred superfluid ring. *Phys. Rev. A*, 88:063633, 2013.

[107] N. Murray, M. Krygier, M. Edwards, K.C. Wright, G.K. Campbell, and C.W. Clark. Probing the circulation of ring-shaped Bose-Einstein condensates. *Phys. Rev. A*, 88:053615, 2013.

[108] S. Eckel, F. Jendrzejewski, A. Kumar, C.J. Lobb, and G.K. Campbell. Interferometric measurement of the current-phase relationship of a superfluid weak link. *Phys. Rev. X*, 4:031052, 2014.

[109] A. Kumar, N. Anderson, W.D. Phillips, S. Eckel, G.K. Campbell, and S. Stringari. Minimally destructive, Doppler measurement of a quantized flow in a ring-shaped Bose-Einstein condensate. *New J. Phys.*, 18:025001, 2016.

[110] S. Eckel, J.G. Lee, F. Jendrzejewski, N. Murray, C.W. Clark, C.J. Lobb, W.D. Phillips, M. Edwards, and G.K. Campbell. Hysteresis in a quantized superfluid 'atomtronic' circuit. *Nature*, 506:200–203, 2014.

[111] R. Mathew, A. Kumar, S. Eckel, F. Jendrzejewski, G.K. Campbell, M. Edwards, and E. Tiesinga. Self-heterodyne detection of the in situ phase of an atomic superconducting quantum interference device. *Phys. Rev. A*, 92:033602, 2015.

[112] C. Ryu, P.W. Blackburn, A.A. Blinova, and M.G. Boshier. Experimental realization of Josephson junctions for an atom SQUID. *Phys. Rev. Lett.*, 111:205301, 2013.

[113] F. Jendrzejewski, S. Eckel, N. Murray, C. Lanier, M. Edwards, C.J. Lobb, and G.K. Campbell. Resistive flow in a weakly interacting Bose-Einstein condensate. *Phys. Rev. Lett.*, 113:045305, 2014.

[114] S. Beattie, S. Moulder, R.J. Fletcher, and Z. Hadzibabic. Persistent currents in spinor condensates. *Phys. Rev. Lett.*, 110:025301, 2013.

[115] S. Burger, K. Bongs, S. Dettmer, W. Ertmer, K. Sengstock, A. Sanpera, G. V. Shlyapnikov, and M. Lewenstein. Dark solitons in Bose-Einstein condensates. *Phys. Rev. Lett.*, 83:5198–5201, 1999.

[116] R. Carmi, E. Polturak, and G. Koren. Observation of spontaneous flux generation in a multi-Josephson-junction loop. *Phys. Rev. Lett.*, 84:4966–4969, 2000.

[117] R. Monaco, J. Mygind, R. J. Rivers, and V. P. Koshelets. Spontaneous fluxoid formation in superconducting loops. *Phys. Rev. B*, 80:180501, 2009.

[118] J. Zhang, J. Beugnon, and S. Nascimbene. Creating fractional quantum Hall states with atomic clusters using light-assisted insertion of angular momentum. *Phys. Rev. A*, 94:043610, 2016.

[119] L. Corman, J.L. Ville, R. Saint-Jalm, M. Aidelsburger, T. Bienaimé, S. Nascimbène, J. Dalibard, and J. Beugnon. Transmission of near-resonant light through a dense slab of cold atoms. *Phys. Rev. A*, 96:053629, 2017.

[120] R. Saint-Jalm, M. Aidelsburger, J.L. Ville, L. Corman, Z. Hadzibabic, D. Delande, S. Nascimbène, N. Cherroret, J. Dalibard, and J. Beugnon. Resonant-light diffusion in a disordered atomic layer. *Phys. Rev. A*, 97:061801, Jun 2018.

[121] S.E. Skipetrov and J.H. Page. Red light for Anderson localization. *New J. Phys.*, 18(2):021001, 2016.

[122] Y. Castin. Bose-Einstein condensates in atomic gases: simple theoretical results. In *Coherent atomic matter waves*, pages 1–136. Springer, 2001.

[123] E. Timmermans. Phase separation of Bose-Einstein condensates. *Phys. Rev. Lett.*, 81:5718–5721, 1998.

[124] C.J. Myatt, E.A. Burt, R.W. Ghrist, E.A. Cornell, and C.E. Wieman. Production of two overlapping Bose-Einstein condensates by sympathetic cooling. *Phys. Rev. Lett.*, 78:586–589, 1997.

[125] D.S. Hall, M.R. Matthews, J.R. Ensher, C.E. Wieman, and E.A. Cornell. Dynamics of component separation in a binary mixture of Bose-Einstein condensates. *Phys. Rev. Lett.*, 81:1539–1542, 1998.

[126] J. Stenger, S. Inouye, D.M. Stamper-Kurn, H.-J. Miesner, A.P. Chikkatur, and W. Ketterle. Spin domains in ground-state Bose–Einstein condensates. *Nature*, 396(6709):345, 1998.

[127] H.-J. Miesner, D.M. Stamper-Kurn, J. Stenger, S. Inouye, A.P. Chikkatur, and W. Ketterle. Observation of metastable states in spinor Bose-Einstein condensates. *Phys. Rev. Lett.*, 82:2228–2231, 1999.

[128] D.M. Stamper-Kurn, H.-J. Miesner, A.P. Chikkatur, S. Inouye, J. Stenger, and W. Ketterle. Quantum tunneling across spin domains in a Bose-Einstein condensate. *Phys. Rev. Lett.*, 83:661–665, 1999.

[129] H.J. Lewandowski, D.M. Harber, D.L. Whitaker, and E.A. Cornell. Observation of anomalous spin-state segregation in a trapped ultracold vapor. *Phys. Rev. Lett.*, 88:070403, 2002.

[130] K.M. Mertes, J.W. Merrill, R. Carretero-González, D.J. Frantzeskakis, P.G. Kevrekidis, and D.S. Hall. Nonequilibrium dynamics and superfluid ring excitations in binary Bose-Einstein condensates. *Phys. Rev. Lett.*, 99:190402, 2007.

[131] R.P. Anderson, C. Ticknor, A.I. Sidorov, and B.V. Hall. Spatially inhomogeneous phase evolution of a two-component Bose-Einstein condensate. *Phys. Rev. A*, 80:023603, 2009.

[132] S. Tojo, Y. Taguchi, Y. Masuyama, T. Hayashi, H. Saito, and T. Hirano. Controlling phase separation of binary Bose-Einstein condensates via mixed-spin-channel Feshbach resonance. *Phys. Rev. A*, 82:033609, 2010.

[133] J. Kronjäger, C. Becker, P. Soltan-Panahi, K. Bongs, and K. Sengstock. Spontaneous pattern formation in an antiferromagnetic quantum gas. *Phys. Rev. Lett.*, 105:090402, 2010.

[134] S. De, D.L. Campbell, R.M. Price, A. Putra, B.M. Anderson, and I.B. Spielman. Quenched binary Bose-Einstein condensates: Spin-domain formation and coarsening. *Phys. Rev. A*, 89:033631, 2014.

[135] Y. Eto, M. Kunimi, H. Tokita, H. Saito, and T. Hirano. Suppression of relative flow by multiple domains in two-component Bose-Einstein condensates. *Phys. Rev. A*, 92:013611, 2015.

[136] S.B. Papp, J.M. Pino, and C.E. Wieman. Tunable miscibility in a dual-species Bose-Einstein condensate. *Phys. Rev. Lett.*, 101:040402, 2008.

[137] D.J. McCarron, H.W. Cho, D.L. Jenkin, M.P. Köppinger, and S.L. Cornish. Dual-species Bose-Einstein condensate of ^{87}Rb and ^{133}Cs. *Phys. Rev. A*, 84:011603, 2011.

[138] L. Wacker, N.B. Jørgensen, D. Birkmose, R. Horchani, W. Ertmer, C. Klempt, N. Winter, J. Sherson, and J.J. Arlt. Tunable dual-species Bose-Einstein condensates of ^{39}K and ^{87}Rb. *Phys. Rev. A*, 92:053602, 2015.

[139] F. Wang, X. Li, D. Xiong, and D. Wang. A double species ^{23}Na and ^{87}Rb Bose–Einstein condensate with tunable miscibility via an interspecies Feshbach resonance. *J. Phys. B: At. Mol. Phys.*, 49(1):015302, 2015.

[140] Y.R.P. Sortais. *Construction d'une fontaine double à atomes froids de* ^{87}Rb *et* ^{133}Cs*; Etude des effets dépendant du nombre d'atomes dans une fontaine*. PhD thesis, Université Pierre et Marie Curie, 2001.

[141] K.E. Strecker, G.B. Partridge, A.G. Truscott, and R.G. Hulet. Formation and propagation of matter-wave soliton trains. *Nature*, 417(6885):150, 2002.

[142] J.H.V. Nguyen, D. Luo, and R.G. Hulet. Formation of matter-wave soliton trains by modulational instability. *Science*, 356(6336):422–426, 2017.

[143] K. Kasamatsu and M. Tsubota. Multiple domain formation induced by modulation instability in two-component Bose-Einstein condensates. *Phys. Rev. Lett.*, 93:100402, 2004.

[144] K. Kasamatsu and M. Tsubota. Modulation instability and solitary-wave formation in two-component Bose-Einstein condensates. *Phys. Rev. A*, 74:013617, 2006.

[145] K. Sasaki, N. Suzuki, and H. Saito. Capillary instability in a two-component Bose-Einstein condensate. *Phys. Rev. A*, 83:053606, 2011.

[146] T. Kadokura, T. Aioi, K. Sasaki, T. Kishimoto, and H. Saito. Rayleigh-Taylor instability in a two-component Bose-Einstein condensate with rotational symmetry. *Phys. Rev. A*, 85:013602, 2012.

[147] H. Takeuchi, N. Suzuki, K. Kasamatsu, H. Saito, and M. Tsubota. Quantum Kelvin-Helmholtz instability in phase-separated two-component Bose-Einstein condensates. *Phys. Rev. B*, 81:094517, 2010.

[148] N. Suzuki, H. Takeuchi, K. Kasamatsu, M. Tsubota, and H. Saito. Crossover between Kelvin-Helmholtz and counter-superflow instabilities in two-component Bose-Einstein condensates. *Phys. Rev. A*, 82:063604, 2010.

[149] K. Sasaki, N. Suzuki, D. Akamatsu, and H. Saito. Rayleigh-Taylor instability and mushroom-pattern formation in a two-component Bose-Einstein condensate. *Phys. Rev. A*, 80:063611, 2009.

[150] K. Sasaki, N. Suzuki, and H. Saito. Dynamics of bubbles in a two-component Bose-Einstein condensate. *Phys. Rev. A*, 83:033602, 2011.

[151] A.P. Chikkatur, A. Görlitz, D.M. Stamper-Kurn, S. Inouye, S. Gupta, and W. Ketterle. Suppression and enhancement of impurity scattering in a Bose-Einstein condensate. *Phys. Rev. Lett.*, 85:483–486, 2000.

[152] M.-S. Chang, C.D. Hamley, M.D. Barrett, J.A. Sauer, K.M. Fortier, W. Zhang, L. You, and M.S. Chapman. Observation of spinor dynamics in optically trapped ^{87}Rb Bose-Einstein condensates. *Phys. Rev. Lett.*, 92:140403, 2004.

[153] H. Schmaljohann, M. Erhard, J. Kronjäger, M. Kottke, S. van Staa, L. Cacciapuoti, J. J. Arlt, K. Bongs, and K. Sengstock. Dynamics of $F = 2$ spinor Bose-Einstein condensates. *Phys. Rev. Lett.*, 92:040402, 2004.

[154] T. Kuwamoto, K. Araki, T. Eno, and T. Hirano. Magnetic field dependence of the dynamics of ^{87}Rb spin-2 Bose-Einstein condensates. *Phys. Rev. A*, 69:063604, 2004.

[155] J. Mur-Petit, M. Guilleumas, A. Polls, A. Sanpera, M. Lewenstein, K. Bongs, and K. Sengstock. Dynamics of $F = 1$ ^{87}Rb condensates at finite temperatures. *Phys. Rev. A*, 73:013629, 2006.

[156] M. Erhard, H. Schmaljohann, J. Kronjäger, K. Bongs, and K. Sengstock. Measurement of a mixed-spin-channel Feshbach resonance in ^{87}Rb. *Phys. Rev. A*, 69:032705, 2004.

[157] E. Nicklas, H. Strobel, T. Zibold, C. Gross, B.A. Malomed, P.G. Kevrekidis, and M.K. Oberthaler. Rabi flopping induces spatial demixing dynamics. *Phys. Rev. Lett.*, 107:193001, 2011.

[158] E. Nicklas, M. Karl, M. Höfer, A. Johnson, W. Muessel, H. Strobel, J. Tomkovič, T. Gasenzer, and M.K. Oberthaler. Observation of scaling in the dynamics of a strongly quenched quantum gas. *Phys. Rev. Lett.*, 115:245301, 2015.

[159] D.M. Stamper-Kurn and M. Ueda. Spinor Bose gases: Symmetries, magnetism, and quantum dynamics. *Rev. Mod. Phys.*, 85:1191–1244, 2013.

[160] A.E. Leanhardt, Y. Shin, D. Kielpinski, D.E. Pritchard, and W. Ketterle. Coreless vortex formation in a spinor Bose-Einstein condensate. *Phys. Rev. Lett.*, 90:140403, 2003.

[161] L.S. Leslie, A. Hansen, K.C. Wright, B.M. Deutsch, and N.P. Bigelow. Creation and detection of skyrmions in a Bose-Einstein condensate. *Phys. Rev. Lett.*, 103:250401, 2009.

[162] J.-Y. Choi, W.J. Kwon, and Y.I. Shin. Observation of topologically stable 2D skyrmions in an antiferromagnetic spinor Bose-Einstein condensate. *Phys. Rev. Lett.*, 108:035301, 2012.

[163] S.W. Seo, S. Kang, W.J. Kwon, and Y.-I. Shin. Half-quantum vortices in an antiferromagnetic spinor Bose-Einstein condensate. *Phys. Rev. Lett.*, 115:015301, 2015.

[164] S.W. Seo, W.J. Kwon, S. Kang, and Y.-I. Shin. Collisional dynamics of half-quantum vortices in a spinor Bose-Einstein condensate. *Phys. Rev. Lett.*, 116:185301, 2016.

[165] M. Tylutki, L.P. Pitaevskii, A. Recati, and S. Stringari. Confinement and precession of vortex pairs in coherently coupled Bose-Einstein condensates. *Phys. Rev. A*, 93:043623, 2016.

[166] M. Eto and M. Nitta. Confinement of half-quantized vortices in coherently coupled Bose-Einstein condensates: Simulating quark confinement in a QCD-like theory. *Phys. Rev. A*, 97:023613, 2018.

[167] L.D. Landau and S.I. Pekar. Effective mass of a polaron. *J. Exp. Theor. Phys*, 18:419–423, 1948.

[168] F. Grusdt and E. Demler. New theoretical approaches to Bose polarons. *arXiv:1510.04934*, 2015.

[169] P. Massignan, M. Zaccanti, and G.M. Bruun. Polarons, dressed molecules and itinerant ferromagnetism in ultracold Fermi gases. *Rep. Prog. Phys.*, 77(3):034401, 2014.

[170] A. Schirotzek, C.-H. Wu, A. Sommer, and M.W. Zwierlein. Observation of Fermi polarons in a tunable Fermi liquid of ultracold atoms. *Phys. Rev. Lett.*, 102:230402, 2009.

[171] C. Kohstall, M. Zaccanti, M. Jag, A. Trenkwalder, P. Massignan, G.M. Bruun, F. Schreck, and R. Grimm. Metastability and coherence of repulsive polarons in a strongly interacting Fermi mixture. *Nature*, 485(7400):615, 2012.

[172] M. Koschorreck, D. Pertot, E. Vogt, B. Fröhlich, M. Feld, and M. Köhl. Attractive and repulsive Fermi polarons in two dimensions. *Nature*, 485(7400):619, 2012.

[173] R. Scelle, T. Rentrop, A. Trautmann, T. Schuster, and M.K. Oberthaler. Motional coherence of fermions immersed in a Bose gas. *Phys. Rev. Lett.*, 111:070401, 2013.

[174] B. Gadway, D. Pertot, R. Reimann, and D. Schneble. Superfluidity of interacting bosonic mixtures in optical lattices. *Phys. Rev. Lett.*, 105:045303, 2010.

[175] T. Fukuhara, A. Kantian, M. Endres, M. Cheneau, P. Schauß, S. Hild, D. Bellem, U. Schollwöck, T. Giamarchi, C. Gross, I. Bloch, and S. Kuhr. Quantum dynamics of a mobile spin impurity. *Nat. Phys.*, 9(4):235, 2013.

[176] D. Chen, C. Meldgin, and B. DeMarco. Bath-induced band decay of a Hubbard lattice gas. *Phys. Rev. A*, 90:013602, 2014.

[177] S. Palzer, C. Zipkes, C. Sias, and M. Köhl. Quantum transport through a Tonks-Girardeau gas. *Phys. Rev. Lett.*, 103:150601, 2009.

[178] J. Catani, G. Lamporesi, D. Naik, M. Gring, M. Inguscio, F. Minardi, A. Kantian, and T. Giamarchi. Quantum dynamics of impurities in a one-dimensional Bose gas. *Phys. Rev. A*, 85:023623, 2012.

[179] T. Rentrop, A. Trautmann, F. A. Olivares, F. Jendrzejewski, A. Komnik, and M.K. Oberthaler. Observation of the phononic Lamb shift with a synthetic vacuum. *Phys. Rev. X*, 6:041041, 2016.

[180] N.B. Jørgensen, L. Wacker, K.T. Skalmstang, M.M. Parish, J. Levinsen, R.S. Christensen, G.M. Bruun, and J.J. Arlt. Observation of attractive and repulsive polarons in a Bose-Einstein condensate. *Phys. Rev. Lett.*, 117:055302, 2016.

[181] M.-G. Hu, M.J. Van de Graaff, D. Kedar, J.P. Corson, E.A. Cornell, and D.S. Jin. Bose polarons in the strongly interacting regime. *Phys. Rev. Lett.*, 117:055301, 2016.

[182] A. Lampo, S.H. Lim, M.A. García-March, and M. Lewenstein. Bose polaron as an instance of quantum Brownian motion. *Quantum*, 1:30, 2017.

[183] J. Bonart and L.F. Cugliandolo. From nonequilibrium quantum Brownian motion to impurity dynamics in one-dimensional quantum liquids. *Phys. Rev. A*, 86:023636, 2012.

[184] P. Massignan, A. Lampo, J. Wehr, and M. Lewenstein. Quantum Brownian motion with inhomogeneous damping and diffusion. *Phys. Rev. A*, 91:033627, 2015.

[185] J. Levinsen, M.M. Parish, R.S. Christensen, J.J. Arlt, and G.M. Bruun. Finite-temperature behavior of the Bose polaron. *Phys. Rev. A*, 96:063622, 2017.

[186] N. Spethmann, F. Kindermann, S. John, C. Weber, D. Meschede, and A. Widera. Dynamics of single neutral impurity atoms immersed in an ultracold gas. *Phys. Rev. Lett.*, 109:235301, 2012.

[187] M. Hohmann, F. Kindermann, T. Lausch, D. Mayer, F. Schmidt, E. Lutz, and A. Widera. Individual tracer atoms in an ultracold dilute gas. *Phys. Rev. Lett.*, 118:263401, 2017.

[188] F. Schmidt, D. Mayer, Q. Bouton, D. Adam, T. Lausch, N. Spethmann, and A. Widera. Quantum spin dynamics of individual neutral impurities coupled to a Bose-Einstein condensate. *arXiv:1802.08702*, 2018.

[189] D. Mayer, F. Schmidt, D. Adam, S. Haupt, J. Koch, T. Lausch, J. Nettersheim, Q. Bouton, and A. Widera. Controlled doping of a bosonic quantum gas with single neutral atoms. *arXiv:1805.01313*, 2018.

[190] W.S. Bakr, J. I Gillen, A. Peng, S. Fölling, and M. Greiner. A quantum gas microscope for detecting single atoms in a Hubbard-regime optical lattice. *Nature*, 462(7269):74, 2009.

[191] J.F. Sherson, C. Weitenberg, M. Endres, M. Cheneau, I. Bloch, and S. Kuhr. Single-atom-resolved fluorescence imaging of an atomic Mott insulator. *Nature*, 467(7311):68, 2010.

[192] M. Miranda, R. Inoue, Y. Okuyama, A. Nakamoto, and M. Kozuma. Site-resolved imaging of ytterbium atoms in a two-dimensional optical lattice. *Phys. Rev. A*, 91:063414, 2015.

[193] I. Boettcher and M. Holzmann. Quasi-long-range order in trapped two-dimensional Bose gases. *Phys. Rev. A*, 94:011602, 2016.

[194] G. Dagvadorj, J.M. Fellows, S. Matyjaśkiewicz, F.M. Marchetti, I. Carusotto, and M.H. Szymańska. Nonequilibrium phase transition in a two-dimensional driven open quantum system. *Phys. Rev. X*, 5:041028, 2015.

[195] E. Altman, L.M. Sieberer, L. Chen, S. Diehl, and J. Toner. Two-dimensional superfluidity of exciton polaritons requires strong anisotropy. *Phys. Rev. X*, 5:011017, 2015.

[196] K. Schwab, E.A. Henriksen, J.M. Worlock, and M.L. Roukes. Measurement of the quantum of thermal conductance. *Nature*, 404(6781):974, 2000.

[197] B.J. van Wees, H. van Houten, C.W.J. Beenakker, J.G. Williamson, L.P. Kouwenhoven, D. van der Marel, and C.T. Foxon. Quantized conductance of point contacts in a two-dimensional electron gas. *Phys. Rev. Lett.*, 60:848–850, 1988.

[198] D. Stadler, S. Krinner, J. Meineke, J.-P. Brantut, and T. Esslinger. Observing the drop of resistance in the flow of a superfluid Fermi gas. *Nature*, 491(7426):736, 2012.

[199] J.-P. Brantut, J. Meineke, D. Stadler, S. Krinner, and T. Esslinger. Conduction of ultracold fermions through a mesoscopic channel. *Science*, 337(6098):1069–1071, 2012.

[200] S. Krinner, T. Esslinger, and J.P. Brantut. Two-terminal transport measurements with cold atoms. *J. Phys. Condens. Matter*, 29(34):343003, 2017.

[201] J.-P. Brantut, C. Grenier, J. Meineke, D. Stadler, S. Krinner, C. Kollath, T. Esslinger, and A. Georges. A thermoelectric heat engine with ultracold atoms. *Science*, 342(6159):713–715, 2013.

[202] S. Krinner, D. Stadler, J. Meineke, J.-P. Brantut, and T. Esslinger. Superfluidity with disorder in a thin film of quantum gas. *Phys. Rev. Lett.*, 110:100601, 2013.

[203] S. Krinner, D. Stadler, D. Husmann, J.-P. Brantut, and T. Esslinger. Observation of quantized conductance in neutral matter. *Nature*, 517(7532):64, 2015.

[204] S. Krinner, M. Lebrat, D. Husmann, C. Grenier, J.-P. Brantut, and T. Esslinger. Mapping out spin and particle conductances in a quantum point contact. *Proc. Natl. Acad. Sci.*, 113(29):8144–8149, 2016.

[205] S. Häusler, S. Nakajima, M. Lebrat, D. Husmann, S. Krinner, T. Esslinger, and J.-P. Brantut. Scanning gate microscope for cold atomic gases. *Phys. Rev. Lett.*, 119:030403, 2017.

[206] M. Lebrat, P. Grišins, D. Husmann, S. Häusler, L. Corman, T. Giamarchi, J.-P. Brantut, and T. Esslinger. Band and correlated insulators of cold fermions in a mesoscopic lattice. *Phys. Rev. X*, 8:011053, 2018.

[207] D. Husmann, S. Uchino, S. Krinner, M. Lebrat, T. Giamarchi, T. Esslinger, and J.-P. Brantut. Connecting strongly correlated superfluids by a quantum point contact. *Science*, 350(6267):1498–1501, 2015.

[208] G. Valtolina, A. Burchianti, A. Amico, E. Neri, K. Xhani, J.A. Seman, A. Trombettoni, A. Smerzi, M. Zaccanti, M. Inguscio, and G. Roati. Josephson effect in fermionic superfluids across the BEC-BCS crossover. *Science*, 350(6267):1505–1508, 2015.

[209] A. Burchianti, F. Scazza, A. Amico, G. Valtolina, J.A. Seman, C. Fort, M. Zaccanti, M. Inguscio, and G. Roati. Connecting dissipation and phase slips in a Josephson junction between fermionic superfluids. *Phys. Rev. Lett.*, 120:025302, 2018.

[210] D.J. Papoular, G. Ferrari, L.P. Pitaevskii, and S. Stringari. Increasing quantum degeneracy by heating a superfluid. *Phys. Rev. Lett.*, 109:084501, 2012.

[211] D.J. Papoular, L.P. Pitaevskii, and S. Stringari. Fast thermalization and Helmholtz oscillations of an ultracold Bose gas. *Phys. Rev. Lett.*, 113(17):170601, 2014.

[212] D.P. Simpson, D.M. Gangardt, I.V. Lerner, and P. Krüger. One-dimensional transport of bosons between weakly linked reservoirs. *Phys. Rev. Lett.*, 112:100601, 2014.

[213] D.J. Papoular, L.P. Pitaevskii, and S. Stringari. Quantized conductance through the quantum evaporation of bosonic atoms. *Phys. Rev. A*, 94(2):023622, 2016.

[214] S. Eckel, Jeffrey G. Lee, F. Jendrzejewski, C. J. Lobb, G. K. Campbell, and W. T. Hill. Contact resistance and phase slips in mesoscopic superfluid-atom transport. *Phys. Rev. A*, 93:063619, 2016.

[215] S. Datta. *Quantum transport: atom to transistor*. Cambridge University Press, 2005.

[216] L.G.C. Rego and G. Kirczenow. Quantized thermal conductance of dielectric quantum wires. *Phys. Rev. Lett.*, 81:232–235, 1998.

[217] T. Jeltes, J.M. McNamara, W. Hogervorst, W. Vassen, V. Krachmalnicoff, M. Schellekens, A. Perrin, H. Chang, D. Boiron, A. Aspect, and C.I. Westbrook. Comparison of the Handbury Brown-Twiss effect for bosons and fermions. *Nature*, 445:402–405, 2007.

[218] A. Griesmaier, J. Werner, S. Hensler, J. Stuhler, and T. Pfau. Bose-Einstein condensation of Chromium. *Phys. Rev. Lett.*, 94:160401, 2005.

[219] Q. Beaufils, R. Chicireanu, T. Zanon, B. Laburthe-Tolra, E. Marechal, L. Vernac, J.-C. Keller, and O. Gorceix. All-Optical Production of Chromium Bose-Einstein Condensates. *Phys. Rev. A*, 77(6):061601, 2008.

[220] M. Lu, N. Burdick, S. Youn, and B. Lev. Strongly dipolar Bose-Einstein condensate of Dysprosium. *Phys. Rev. Lett.*, 107:190401, 2011.

[221] K. Aikawa, A. Frisch, M. Mark, S. Baier, A. Rietzler, R. Grimm, and F. Ferlaino. Bose-Einstein condensation of Erbium. *Phys. Rev. Lett.*, 108:210401, 2012.

[222] Y. de Escobar, P. Mickelson, M. Yan, B. DeSalvo, S. Nagel, and T. Killian. Bose-Einstein condensation of ^{84}Sr. *Phys. Rev. Lett.*, 103:200402, 2009.

[223] S. Stellmer, M. Tey, B. Huang, R. Grimm, and F. Schreck. Bose-Einstein condensation of Strontium. *Phys. Rev. Lett.*, 103:200401, 2009.

[224] S. Kraft, F. Vogt, O. Appel, F. Riehle, and U. Sterr. Bose-Einstein condensation of alkaline earth atoms: ^{40}Ca. *Phys. Rev. Lett.*, 103:130401, 2009.

[225] Y. Takasu, K. Maki, K. Komori, T. Takano, K. Honda, M. Kumakura, T. Yabuzaki, and Y. Takahashi. Spin-singlet Bose-Einstein condensation of two-electron atoms. *Phys. Rev. Lett.*, 91:040404, 2003.

[226] S. Dörscher, A. Thobe, B. Hundt, A. Kochanke, R. Le Targat, P. Windpassinger, C. Becker, and K. Sengstock. Creation of quantum-degenerate gases of ytterbium in a compact 2D-/3D-magneto-optical trap setup. *Rev. Sci. Instrum.*, 84(4):043109, 2013.

[227] M. Miranda, A. Nakamoto, Y. Okuyama, A. Noguchi, M. Ueda, and M. Kozuma. All-optical transport and compression of ytterbium atoms into the surface of a solid immersion lens. *Phys. Rev. A*, 86:063615, 2012.

[228] N. Poli, C. W. Oates, P. Gill, and G. M. Tino. Optical atomic clocks. *Rivista del nuovo cimento*, 36(12):555–624, 2013.

[229] A. Gorshkov, A. Rey, A. Daley, M. Boyd, J. Ye, P. Zoller, and M. Lukin. Alkaline-earth-metal atoms as few-qubit quantum registers. *Phys. Rev. Lett.*, 102:110503, 2009.

[230] L. F. Livi, G. Cappellini, M. Diem, L. Franchi, C. Clivati, M. Frittelli, F. Levi, D. Calonico, J. Catani, M. Inguscio, and L. Fallani. Synthetic dimensions and spin-orbit coupling with an optical clock transition. *Phys. Rev. Lett.*, 117:220401, 2016.

[231] S. Kolkowitz, S.L. Bromley, T. Bothwell, M.L. Wall, G.E. Marti, A.P. Koller, X. Zhang, A.M. Rey, and J. Ye. Spin–orbit-coupled fermions in an optical lattice clock. *Nature*, 542(7639):66, 2017.

[232] S. Taie, R. Yamazaki, and Y. Sugawa, S.and Takahashi. An SU(6) Mott insulator of an atomic Fermi gas realized by large-spin Pomeranchuk cooling. *Nat. Phys.*, 8(11):825, 2012.

[233] G. Pagano, M. Mancini, G. Cappellini, P. Lombardi, F. Schäfer, H. Hu, X.-J. Liu, J. Catani, C. Sias, M. Inguscio, and L. Fallani. A one-dimensional liquid of fermions with tunable spin. *Nat. Phys.*, 10(3):198, 2014.

[234] C. Hofrichter, L. Riegger, F. Scazza, M. Höfer, D. Rio Fernandes, I. Bloch, and S. Fölling. Direct probing of the Mott crossover in the SU(N) Fermi-Hubbard model. *Phys. Rev. X*, 6:021030, 2016.

[235] M. Scholl. *Probing an Ytterbium Bose-Einstein condensate using an ultranarrow optical line : towards artificial gauge fields in optical lattices*. PhD thesis, Université Pierre et Marie Curie, 2014.

[236] A. Dareau. *Manipulation cohérente d'un condensat de Bose-Einstein d'ytterbium sur la transition "d'horloge" : de la spectroscopie au magnétisme artificiel*. PhD thesis, Ecole Normale Supérieure, 2015.

[237] D.G. Fried, T.C. Killian, L. Willmann, D. Landhuis, S.C. Moss, D. Kleppner, and T.J. Greytak. Bose-Einstein condensation of atomic Hydrogen. *Phys. Rev. Lett.*, 81:3811–3814, 1998.

[238] G.E. Marti, R.B. Hutson, A. Goban, S.L. Campbell, N. Poli, and J. Ye. Imaging optical frequencies with 100 μHz precision and 1.1 μm resolution. *Phys. Rev. Lett.*, 120:103201, 2018.

[239] R. Bouganne, M. Bosch Aguilera, A. Dareau, E. Soave, J. Beugnon, and F. Gerbier. Clock spectroscopy of interacting bosons in deep optical lattices. *New J. Phys.*, 19(11):113006, 2017.

[240] M. Kitagawa, K. Enomoto, K. Kasa, Y. Takahashi, R. Ciuryło, P. Naidon, and P.S. Julienne. Two-color photoassociation spectroscopy of Ytterbium atoms and the precise determinations of s-wave scattering lengths. *Phys. Rev. A*, 77:012719, 2008.

[241] L. Franchi, L.F. Livi, G. Cappellini, G. Binella, M. Inguscio, J. Catani, and L. Fallani. State-dependent interactions in ultracold ^{174}Yb probed by optical clock spectroscopy. *New J. Phys.*, 19(10):103037, 2017.

[242] A. Goban, R.B. Hutson, G.E. Marti, S.L. Campbell, M.A. Perlin, P.S. Julienne, J.P. D'Incao, A.M. Rey, and J. Ye. Emergence of multi-body interactions in few-atom sites of a fermionic lattice clock. *arXiv:1803.11282*, 2018.

[243] M. Bosch Aguilera, R. Bouganne, A. Dareau, M. Scholl, Q. Beaufil, J. Beugnon, and F. Gerbier. Non-linear relaxation of interacting bosons coherently driven on a narrow optical transition. *arXiv:18XX.XXXX*, 2018.

[244] A. Yamaguchi, S. Uetake, S. Kato, H. Ito, and Y. Takahashi. High-resolution laser spectroscopy of a Bose–Einstein condensate using the ultranarrow magnetic quadrupole transition. *New J. Phys.*, 12(10):103001, 2010.

[245] R. van Rooij, J.S. Borbely, J. Simonet, M.D. Hoogerland, K. S.E. Eikema, R.A. Rozendaal, and W. Vassen. Frequency metrology in quantum degenerate helium: Direct measurement of the $2^3S_1 \rightarrow 2^1S_0$ transition. *Science*, 333(6039):196–198, 2011.

[246] R.P.M.J.W. Notermans, R.J. Rengelink, and W. Vassen. Comparison of spectral linewidths for quantum degenerate bosons and fermions. *Phys. Rev. Lett.*, 117:213001, 2016.

[247] D.J. Thouless, M. Kohmoto, M.P. Nightingale, and M. Den Nijs. Quantized Hall conductance in a two-dimensional periodic potential. *Phys. Rev. Lett.*, 49(6):405, 1982.

[248] R.B. Laughlin. Anomalous quantum Hall effect: An incompressible quantum fluid with fractionally charged excitations. *Phys. Rev. Lett.*, 50:1395–1398, 1983.

[249] G. Moore and N. Read. Nonabelions in the fractional quantum Hall effect. *Nucl. Phys. B*, 360(2-3):362–396, 1991.

[250] V. Bretin, S. Stock, Y. Seurin, and J. Dalibard. Fast rotation of a Bose-Einstein condensate. *Phys. Rev. Lett.*, 92:050403, 2004.

[251] V. Schweikhard, I. Coddington, P. Engels, V.P. Mogendorff, and E.A. Cornell. Rapidly rotating Bose-Einstein condensates in and near the lowest Landau level. *Phys. Rev. Lett.*, 92:040404, 2004.

[252] G. Juzeliūnas and P. Öhberg. Slow light in degenerate Fermi gases. *Phys. Rev. Lett.*, 93:033602, 2004.

[253] K.J. Günter, M. Cheneau, T. Yefsah, S.P. Rath, and J. Dalibard. Practical scheme for a light-induced gauge field in an atomic Bose gas. *Phys. Rev. A*, 79:011604, 2009.

[254] Y.-J. Lin, R.L. Compton, K. Jimenez-Garcia, J.V. Porto, and I.B. Spielman. Synthetic magnetic fields for ultracold neutral atoms. *Nature*, 462(7273):628, 2009.

[255] M. Aidelsburger, S. Nascimbene, and N. Goldman. Artificial gauge fields in materials and engineered systems. *arXiv:1710.00851*, 2017.

[256] T. Ozawa, H.M. Price, A. Amo, N. Goldman, M. Hafezi, L. Lu, M. Rechtsman, D. Schuster, J. Simon, O. Zilberberg, and I. Carusotto. Topological photonics. *arXiv:1802.04173*, 2018.

[257] W.P. Su, J.R. Schrieffer, and A.J. Heeger. Solitons in polyacetylene. *Phys. Rev. Lett.*, 42:1698–1701, 1979.

[258] M. Atala, M. Aidelsburger, J.T. Barreiro, D. Abanin, T. Kitagawa, E. Demler, and I. Bloch. Direct measurement of the Zak phase in topological Bloch bands. *Nat. Phys.*, 9(12):795, 2013.

[259] A. Celi, P. Massignan, J. Ruseckas, N. Goldman, I. B. Spielman, G. Juzeliūnas, and M. Lewenstein. Synthetic gauge fields in synthetic dimensions. *Phys. Rev. Lett.*, 112:043001, 2014.

[260] B.K. Stuhl, H.-I. Lu, L.M. Aycock, D. Genkina, and I.B. Spielman. Visualizing edge states with an atomic Bose gas in the quantum Hall regime. *Science*, 349(6255):1514–1518, 2015.

[261] M. Mancini, G. Pagano, G. Cappellini, L. Livi, M. Rider, J. Catani, C. Sias, P. Zoller, M. Inguscio, M. Dalmonte, and L. Fallani. Observation of chiral edge states with neutral fermions in synthetic Hall ribbons. *Science*, 349(6255):1510–1513, 2015.

[262] D. Genkina, L.M. Aycock, H.-I. Lu, A.M. Pineiro, M. Lu, and I.B. Spielman. Imaging topology of Hofstadter ribbons. *arXiv:1804.06345*, 2018.

[263] M.C. Strinati, E. Cornfeld, D. Rossini, S. Barbarino, M. Dalmonte, R. Fazio, E. Sela, and L. Mazza. Laughlin-like states in bosonic and fermionic atomic synthetic ladders. *Phys. Rev. X*, 7:021033, 2017.

[264] M.C. Strinati, F. Gerbier, and L. Mazza. Spin-gap spectroscopy in a bosonic flux ladder. *New J. Phys.*, 20(1):015004, 2018.

[265] D.J. Thouless. Quantization of particle transport. *Phys. Rev. B*, 27:6083–6087, 1983.

[266] M. Lohse, C. Schweizer, O. Zilberberg, M. Aidelsburger, and I. Bloch. A Thouless quantum pump with ultracold bosonic atoms in an optical superlattice. *Nat. Phys.*, 12(4):350, 2016.

[267] S. Nakajima, T. Tomita, S. Taie, T. Ichinose, H. Ozawa, L. Wang, M. Troyer, and Y. Takahashi. Topological Thouless pumping of ultracold fermions. *Nat. Phys.*, 12(4):296, 2016.

[268] F.D.M. Haldane. Model for a Quantum Hall effect without Landau levels: Condensed-matter realization of the "parity anomaly". *Phys. Rev. Lett.*, 61:2015–2018, 1988.

[269] M. Aidelsburger, M. Atala, S. Nascimbène, S. Trotzky, Y.-A. Chen, and I. Bloch. Experimental realization of strong effective magnetic fields in an optical lattice. *Phys. Rev. Lett.*, 107:255301, 2011.

[270] H. Miyake, G.A. Siviloglou, C.J. Kennedy, W.C. Burton, and W. Ketterle. Realizing the Harper Hamiltonian with laser-assisted tunneling in optical lattices. *Phys. Rev. Lett.*, 111:185302, 2013.

[271] M. Aidelsburger, M. Atala, M. Lohse, J. T. Barreiro, B. Paredes, and I. Bloch. Realization of the Hofstadter Hamiltonian with ultracold atoms in optical lattices. *Phys. Rev. Lett.*, 111:185301, 2013.

[272] M. Aidelsburger, M. Lohse, C. Schweizer, M. Atala, J.T. Barreiro, S. Nascimbene, N.R. Cooper, I. Bloch, and N. Goldman. Measuring the Chern number of Hofstadter bands with ultracold bosonic atoms. *Nat. Phys.*, 11(2):162, 2015.

[273] H. Lignier, C. Sias, D. Ciampini, Y. Singh, A. Zenesini, O. Morsch, and E. Arimondo. Dynamical control of matter-wave tunneling in periodic potentials. *Phys. Rev. Lett.*, 99:220403, 2007.

[274] E. Kierig, U. Schnorrberger, A. Schietinger, J. Tomkovic, and M.K. Oberthaler. Single-particle tunneling in strongly driven double-well potentials. *Phys. Rev. Lett.*, 100:190405, 2008.

[275] J. Struck, C. Ölschläger, M. Weinberg, P. Hauke, J. Simonet, A. Eckardt, M. Lewenstein, K. Sengstock, and P. Windpassinger. Tunable gauge potential for neutral and spinless particles in driven optical lattices. *Phys. Rev. Lett.*, 108:225304, 2012.

[276] J. Struck, M. Weinberg, C. Ölschläger, P. Windpassinger, J. Simonet, K. Sengstock, R. Höppner, P. Hauke, A. Eckardt, M. Lewenstein, and L. Mathey. Engineering Ising-XY spin-models in a triangular lattice using tunable artificial gauge fields. *Nat. Phys.*, 9(11):738, 2013.

[277] G. Jotzu, M. Messer, R. Desbuquois, M. Lebrat, T. Uehlinger, D. Greif, and T. Esslinger. Experimental realization of the topological Haldane model with ultracold fermions. *Nature*, 515(7526):237, 2014.

[278] N. Fläschner, B.S. Rem, M. Tarnowski, D. Vogel, D.-S. Lühmann, K. Sengstock, and C. Weitenberg. Experimental reconstruction of the Berry curvature in a Floquet Bloch band. *Science*, 352(6289):1091–1094, 2016.

[279] M. Lohse, C. Schweizer, H.M. Price, O. Zilberberg, and I. Bloch. Exploring 4D quantum Hall physics with a 2D topological charge pump. *Nature*, 553(7686):55, 2018.

[280] Y.-J. Lin, K. Jiménez-García, and I.B. Spielman. Spin–orbit-coupled Bose–Einstein condensates. *Nature*, 471(7336):83, 2011.

[281] P. Wang, Z.-Q. Yu, Z. Fu, J. Miao, L. Huang, S. Chai, H. Zhai, and J. Zhang. Spin-orbit coupled degenerate Fermi gases. *Phys. Rev. Lett.*, 109:095301, 2012.

[282] J. Li, W. Huang, B. Shteynas, S. Burchesky, F.C. Top, E. Su, J. Lee, A.O. Jamison, and W. Ketterle. Spin-orbit coupling and spin textures in optical superlattices. *Phys. Rev. Lett.*, 117:185301, 2016.

[283] Z. Wu, L. Zhang, W. Sun, X.-T. Xu, B.-Z. Wang, S.-C. Ji, Y. Deng, S. Chen, X.-J. Liu, and J.-W. Pan. Realization of two-dimensional spin-orbit coupling for Bose-Einstein condensates. *Science*, 354(6308):83–88, 2016.

[284] W. Sun, B.-Z. Wang, X.-T. Xu, C.-R. Yi, L. Zhang, Z. Wu, Y. Deng, X.-J. Liu, S. Chen, and J.-W. Pan. Long-lived 2D spin-orbit coupled topological Bose gas. *arXiv:1710.00717*, 2017.

[285] W. Sun, C.-R. Yi, B.-Z. Wang, W.-W. Zhang, B.C. Sanders, X.-T. Xu, Z.-Y. Wang, J. Schmiedmayer, Y. Deng, X.-J. Liu, S. Chen, and J.-W. Pan. Uncover topology by quantum quench dynamics. *arXiv:1804.08226*, 2018.

[286] N.R. Cooper. Optical flux lattices for ultracold atomic gases. *Phys. Rev. Lett.*, 106:175301, 2011.

[287] N.R. Cooper and J. Dalibard. Reaching fractional quantum Hall states with optical flux lattices. *Phys. Rev. Lett.*, 110:185301, 2013.

[288] S. Choudhury and E.J. Mueller. Stability of a Floquet Bose-Einstein condensate in a one-dimensional optical lattice. *Phys. Rev. A*, 90:013621, 2014.

[289] T. Bilitewski and N.R. Cooper. Scattering theory for Floquet-Bloch states. *Phys. Rev. A*, 91:033601, 2015.

[290] M. Reitter, J. Näger, K. Wintersperger, C. Sträter, I. Bloch, A. Eckardt, and U. Schneider. Interaction dependent heating and atom loss in a periodically driven optical lattice. *Phys. Rev. Lett.*, 119:200402, 2017.

[291] C.J. Kennedy, W.C. Burton, W.C. Chung, and W. Ketterle. Observation of Bose-Einstein condensation in a strong synthetic magnetic field. *Nat. Phys.*, 11(10):859–864, 2015.

[292] D.R. Hofstadter. Energy levels and wave functions of Bloch electrons in rational and irrational magnetic fields. *Phys. Rev. B*, 14:2239–2249, 1976.

[293] H.M. Price and N.R. Cooper. Mapping the Berry curvature from semiclassical dynamics in optical lattices. *Phys. Rev. A*, 85:033620, 2012.

[294] L. Duca, T. Li, M. Reitter, I. Bloch, M. Schleier-Smith, and U. Schneider. An Aharonov-Bohm interferometer for determining Bloch band topology. *Science*, 347(6219):288–292, 2014.

[295] T. Li, L. Duca, M. Reitter, F. Grusdt, E. Demler, M. Endres, M. Schleier-Smith, I. Bloch, and U. Schneider. Bloch state tomography using Wilson lines. *Science*, 352(6289):1094–1097, 2016.

[296] N. Goldman, J. Dalibard, A. Dauphin, F. Gerbier, M. Lewenstein, P. Zoller, and I.B. Spielman. Direct imaging of topological edge states in cold-atom systems. *PNAS*, 110(17):6736–6741, 2013.

[297] N. Goldman, J. Beugnon, and F. Gerbier. Detecting chiral edge states in the Hofstadter optical lattice. *Phys. Rev. Lett.*, 108(25):255303, 2012.

[298] N. Goldman, J. Beugnon, and F. Gerbier. Identifying topological edge states in 2D optical lattices using light scattering. *Eur. Phys. J. Special Topics*, 217(1):135–152, 2013.

[299] N. Goldman, G. Juzeliūnas, P. Öhberg, and I.B. Spielman. Light-induced gauge fields for ultracold atoms. *Rep. Prog. Phys.*, 77(12):126401, 2014.

[300] J.R. Abo-Shaeer, C. Raman, J.M. Vogels, and W. Ketterle. Observation of vortex lattices in Bose-Einstein condensates. *Science*, 292(5516):476–479, 2001.

[301] S. Tung, V. Schweikhard, and E.A. Cornell. Observation of vortex pinning in Bose-Einstein condensates. *Phys. Rev. Lett.*, 97:240402, 2006.

[302] R.O. Umucalilar and E.J. Mueller. Fractional quantum Hall states in the vicinity of Mott plateaus. *Phys. Rev. A*, 81:053628, 2010.

[303] S. Fölling, A. Widera, T. Müller, F. Gerbier, and I. Bloch. Formation of spatial shell structure in the superfluid to Mott insulator transition. *Phys. Rev. Lett.*, 97:060403, 2006.

[304] A. Dareau, E. Levy, M. Bosch Aguilera, R. Bouganne, E. Akkermans, F. Gerbier, and J. Beugnon. Revealing the topology of quasicrystals with a diffraction experiment. *Phys. Rev. Lett.*, 119:215304, 2017.

[305] Y.E. Kraus and O. Zilberberg. Topological equivalence between the Fibonacci quasicrystal and the Harper model. *Phys. Rev. Lett.*, 109:116404, 2012.